80-FM-41

JSC-16762

AUG 2 9 1980

Solar Activity Prediction of Sunspot Numbers (Verification)

Predicted Solar Radio Flux

Predicted Geomagnetic Indices A_p and K_p

Mission Planning and Analysis Division

August 1980

NASA

National Aeronautics and Space Administration

Lyndon B. Johnson Space Center
Houston, Texas

80-FM-41

JSC-16762

SHUTTLE PROGRAM

SOLAR ACTIVITY PREDICTION OF SUNSPOT NUMBERS (VERIFICATION)

PREDICTED SOLAR RADIO FLUX
PREDICTED GEOMAGNETIC INDICES A_p AND K_p

By Samuel R. Newman, Software Development Branch

Approved: Elric R McHenry
Elric R. McHenry, Chief
Software Development Branch

Approved: Ronald L. Berry
Ronald L. Berry, Chief
Mission Planning and Analysis Division

Mission Planning and Analysis Division

National Aeronautics and Space Administration

Lyndon B. Johnson Space Center

Houston, Texas

August 1980

CONTENTS

TABLE

FIGURES

FIGURES (Concluded)

1.0 INTRODUCTION

Three studies are presented in this document. The first is a followup of a previous report (ref. 1), which presented a new technique for predicting monthly sunspot numbers over a period of several years (February 1979 to 1989). This followup report presents the result of a subsequent effort to further verify the prediction technique over the period for the maximum epoch of solar cycle 19. The second and third studies presented in this report, respectively, are new techniques and results for predicting solar flux (F10.7 cm) based on two flux/sunspot number models, ascent and descent and geomagnetic activity indices A_p and K_p as a function of sunspot number and solar cycle phase classes.

Orbit lifetime models used within the MPAD generally utilize atmospheric density models that require data specifying a measure of solar flux and the geomagnetic activity index (fig. 1).

2.0 SUNSPOT NUMBER PREDICTION TECHNIQUES

The sunspot number prediction technique by the author and G. G. Johnson (ref. 1), is applied here for additional verification. A different timeframe (years of the solar cycle) was used, which includes the maximum epoch sunspot numbers of solar cycle 19 (largest values observed to date).

3.0 CYCLE 19 SUNSPOT NUMBER PREDICTION

The prediction analysis from (ref. 1) used the solar activity sunspot number historical period (monthly observed values) shown in figure 2 as input to the study. Also included in the document was a prediction verification analysis that used the same sunspot number record but terminated the last input data point in December 1972, allowing actual observed sunspot numbers to be compared with the predicted results (January 1973 to January 1979). The timeframe included sunspot numbers observed just before and after the minimum epoch of cycle 21, June 1976.

This comparison showed highly favorable results for that time period, however, to fully test this prediction technique, it was deemed necessary to make this follow-on study using a different set of conditions; i.e., solar maximum epoch values.

Presented in figure 3 are the observed sunspot numbers from approximately 1943 to 1968, which includes the maximum epoch values this study will predict. The actual input data to the prediction model used are sunspot numbers observed from 1830 to January 1956 (fig. 4). The resulting 10-year sunspot prediction starts in February 1955 and extends to January 1965.

4.0 FINAL RESIDUAL CURVE

By applying the same mathematical and computational technique of reference 1 to the sunspot number record in figure 4, a model composed of 19 spectural lines

was obtained by numerous iterations. Figure 5 shows the final residual curve R19 as a function of month/years with the last value at January 1956. Using the same logic as before, the predicted residual was determined by symmetric extension and is presented in figure 6.

NOTE: The summation of the 19 harmonics of the model with the residual R1' in figure 5 yields the original input sunspot record. Therefore, as pointed out in reference 1, when the extrapolated portion of the residual R19 is summed in a like manner, the result is a prediction of the sunspot numbers for that timeframe.

5.0 COMPARISON OF THE PREDICTED AND OBSERVED SUNSPOT NUMBERS

The predicted sunspot numbers from January 1956 to January 1965 are shown in figure 7 with the actual observed sunspot numbers for comparison purposes. The customary format of presenting these values (all positive) is presented in figure 8.

6.0 SUMMARY OF CYCLE 19 SUNSPOT NUMBER PREDICTION

To summarize the results of the R19 residual study, three plots are shown in figure 9 that include (a) the residual R19 curve alone, (b) the R19 residual curve and extrapolated residual, and (c) sunspot number curve for both predicted and observed values.

NOTE: These predicted sunspot numbers show good overall agreement with the actual observed sunspot numbers. During the maximum epoch of this cycle, the maximum delta sunspot number difference between the predicted and observed values was ($\pm$20) for a given month. However, when considering the entire curve for this timeframe, the predicted values average out to a respectable comparison. Therefore, the results from this R19 study indicate the predicted sunspot numbers for the reference 1 study are acceptable.

7.0 PREDICTED SOLAR FLUX (F10.7)

The predicted solar flux data presented in reference 1 (1979-1989) were smooth F10.7-cm values based on an (sunspot number/flux) empirical relationship using smooth 13-month smooth sunspot numbers as input (fig. 10). The curve in figure 10 is derived from a numerous amount of observed sunspot numbers and flux data without regard for the ascending or descending phases of the solar cycle; i.e., all of the data were included into one large sample. (See reference 1 of reference 1.)

This document presents the effects of the ascending and descending phases of the solar cycle and the two new (sunspot number/flux) models that were derived.

It was noted, when looking at the sunspot number/flux daily or monthly values over a period of time, that a distinction between the ascending and descending values existed and could be identified. The investigation of these data is discussed.

a. Sunspot number and solar flux time history investigated

Over 4000 observed daily sunspot number and flux data samples from 1955 through 1965 (ref. 2) were used for the analysis. To understand the relationship of sunspot numbers to flux values, several plots were generated and are discussed as follows:

Figures 11 and 12 present, respectively, sunspot number and solar flux shows values observed over the 1 ,ear span. The same data (fig. 13) sunspot number as a function of flux values for this same timeframe. This plot shows all of the data samples together without regard to the ascending or descending effect of the phases of the solar cycles. The author investigated the difference between ascent and descent values. Presented in figure 14 are the ascent phase (sunspot number/flux) data extracted out of figure 13 and likewise the descent phase (sunspot number/flux) data shown in figure 15. The next step was to develop the ascent and descent models that were derived by determining an average flux value for a given sunspot number with its associated maximum and minimum values. The maximum and minimum values average out to be slightly less than ±2 sigma. This approach produced the models presented in figures 16 and 17, which are called ascent flux envelope and descent flux envelope, where the average value of each is included with its maximum and minimum expected values, thus determining the envelopes.

b. Comparison of predicted and observed flux (1965-1979)

A test case was generated (fig. 18) using the observed monthly mean sunspot numbers for (1965-1979) with the new models using predicted flux and observed flux for verification. The predicted flux agrees well with the observed flux and confirms the accuracy of the new models.

c. Comparison of predicted flux data (1979-1989)

This section presents various results of both the Johnson Space Center (JSC) and Marshall Space Flight Center (MFSC) predicted flux values for the years (1979-1989). The MSFC data used are from reference 3. Using the JSC predicted sunspot numbers from reference 1 and the new JSC sunspot number/flux models (ascent and descent), a predicted flux envelope was developed and is presented in figure 17. Note that these flux values (maximum, average, and minimum) are predicted monthly mean values and not smooth as in the case for the MSFC prediction techniques. Figure 20 presents the MSFC (5-month smooth) predicted flux envelope from reference 3 for cycle 21 where the maximum represents (97.7), minimum (2.3) and the average (50) percentile predictions, or approximately ±2 sigma values.

The JSC predicted flux was modified from the monthly values to a 5-month curve for comparison purposes with the MSFC 5-month prediction. These data are shown in figure 21 in conjunction with monthly observed flux.

Finally, a summary plot for this flux study is presented in figure 22, which shows the JSC developed ascent and descent sunspot number/flux models and the predicted JSC monthly flux envelope for 1979-1989.

8.0 GEOMAGNETIC INDICES A_p and K_p

Given a particular level of geomagnetic activity measured by the planetary geomagnetic index K_p, the geomagnetic heating (increase in the exospheric temperature above the quiet temperature corresponding to $K_p = 0$), can then be expressed as a function of the invarient magnetic latitude (ref. 4).

a. Definition of A_p and K_p

Excellent descriptions of these indices can be found in reference 5. Here it may be sufficient to say that the index K_p ranks all 3-hour intervals of the Greenwich day according to increasing disturbance (activity) by assigning one of the indices zero (quiet), 1, 2, 3, ... 9 (intense storm). The average of the eight ranges of (ap) per day is the daily amplitude A_p, which can range in value from zero to 400. The relationship between K_p and A_p is presented in figure 23 for conversion purposes.

b. Sunspot number/A_p prediction models

Since the geomagnetic activity A_p or K_p indices predictions are used in orbital lifetime programs along with the predicted solar flux (F10.7 cm) values, the author performed a study to predict values of A_p corresponding to the already defined predicted sunspot numbers of cycle 21 (ref. 1).

To derive suitable models for predicting values of A_p, data were extracted from reference 6, which discussed and presented results of time variations of the geomagnetic activity indices K_p and A_p. Basically, this reference presented K_p and A_p data for the 12 calendar months using various classes in the sunspot cycle for 30 years of data as follows:

Class A - minimum epoch
Class B - ascending
Class C - maximum epoch
Class D - descending

For each class there exists a corresponding monthly A_p index that is the average for all days; the A_pD index (average for 5 disturbed days per month and the A_pQ index that is the average for 5 quiet days per month. To formulate a geomagnetic model for this study, the concept of classes for the sunspot cycle was used similar to the above. However, the author redefined the classes for prediction purposes as shown in figure 24. A description of these classes is presented in table I, and an example of one of the models (class B) is presented in figure 25. Each of the classes has been modeled

as A_pD, A_p and A_pQ as a function of sunspot number as shown in this plot. Therefore, using the predicted sunspot numbers (monthly) from reference 1, which includes solar cycle 21 and part of solar cycle 22, and these geomagnetic models (classes of the sunspot cycle), then predicted values of A_pD, A_p, and A_pQ were obtained for this same timeframe.

c. Comparison of predicted geomagnetic indices

The predicted JSC geomagnetic envelope values of A_pD, A_p and A_pQ from 1979 to 1989 are presented in figure 26.

The predicted MSFC geomagnetic envelope values of A_p from 1979 to 1987 from reference 2 are presented in figure 27. They are 5-month smooth A_p index values where the maximum represents (97.7), minimum (2.3) and average 50-percentile predictions, approximately ± 2 sigma.

Because the MSFC A_p data are based on 5-month smooth values, an additional step was preformed to alter the JSC monthly A_p values to predicted 5-month smooth values. Comparison of the JSC 5-month smooth A_p values with the MSFC 5-month smooth envelope data are presented in figure 28. The JSC data are not as smooth as the MSFC but overall agree favorably. Also included is the JSC 5-month smooth A_p curve imposed on the plot in figure 26.

In summary of these comparisons figure 30 is presented, which shows three separate plot cases. Included are the predicted MSFC 5-month smooth A_p envelope, the JSC monthly A_p envelope, and the same JSC envelope with the imposed MSFC 5-month smooth A_p values plotted as connecting circles.

Because some organizations use K_p instead of A_p as input to their density models, then converting to predicted K_p values is accomplished with little difficulty using the relationship of A_p to K_p already presented in figure 23. Figure 31 presents a plot of the predicted K_p values that were converted from A_p. The data shown are for the MSFC 5-month K_p envelope in conjunction with the JSC 5-month K_p values.

9.0 CONCLUSIONS

This paper deals with three primary subjects: (1) predicted sunspot numbers, (2) predicted solar flux (F10.7 cm), and (3) predicted geomagnetic indices A_p and K_p. The techniques and prediction models for each of these are presented and discussed with numerous plot results.

To best summarize this work, included is a final summary plot (fig. 32), which presents the final predicted results of each of these studies.

10.0 REFERENCES

1. Newman, S. R.; and Johnson, Gordon G.: Solar Activity Prediction of Sunspot Numbers Predicted Solar Radio Flux. JSC IN 80-FM-8, Februarv 1980.

2. Magnetic Data Tape, Solar Activity Data. World Data Center, NOAA, December 1978.

3. Vaughn, William W.: Solar Activity Inputs for Upper Atmosphere Models Used in Orbital Lifetime Estimates. MSFC memorandum ES8A, September 15, 1979.

4. Jacchia, L. G.: Thermospheric Temperature, Density, and Composition: New Models. Smithsoniam Astrophysical Observatory, Special Report 375, March 15, 1977.

5. NOAA: Solar-Geophysical Data Explanation of Data Reports. No. 402 (Supplement), February 1978.

6. Bartels, J.: Discussion of Time Variations of Geomagnetic Activity, Indices K_p and A_p, 1932-1961. IAGA Bulletin No. 19, January 1963.

TABLE I.- SUBDIVISION OF CLASSES FOR A TYPICAL SOLAR CYCLE

Class	Description
A	Immediately before minimum epoch (sunspot number range is approximately: 5 -12)
A'	Immediately after minimum epoch (sunspot number range is approximately: 2 -12)
A+	After class A' (to sunspot number approximately: 35)
B	Ascending (sunspot number range to approximately: 93)
C	Ascending maximum epoch (sunspot number range to approximately: 100)
D	Descending maximum epoch (sunspot number range to approximately: 100)
E	Descending (sunspot number range to approximately: 26)
E'	Descending before class A (to sunspot number approximately: 25.9)

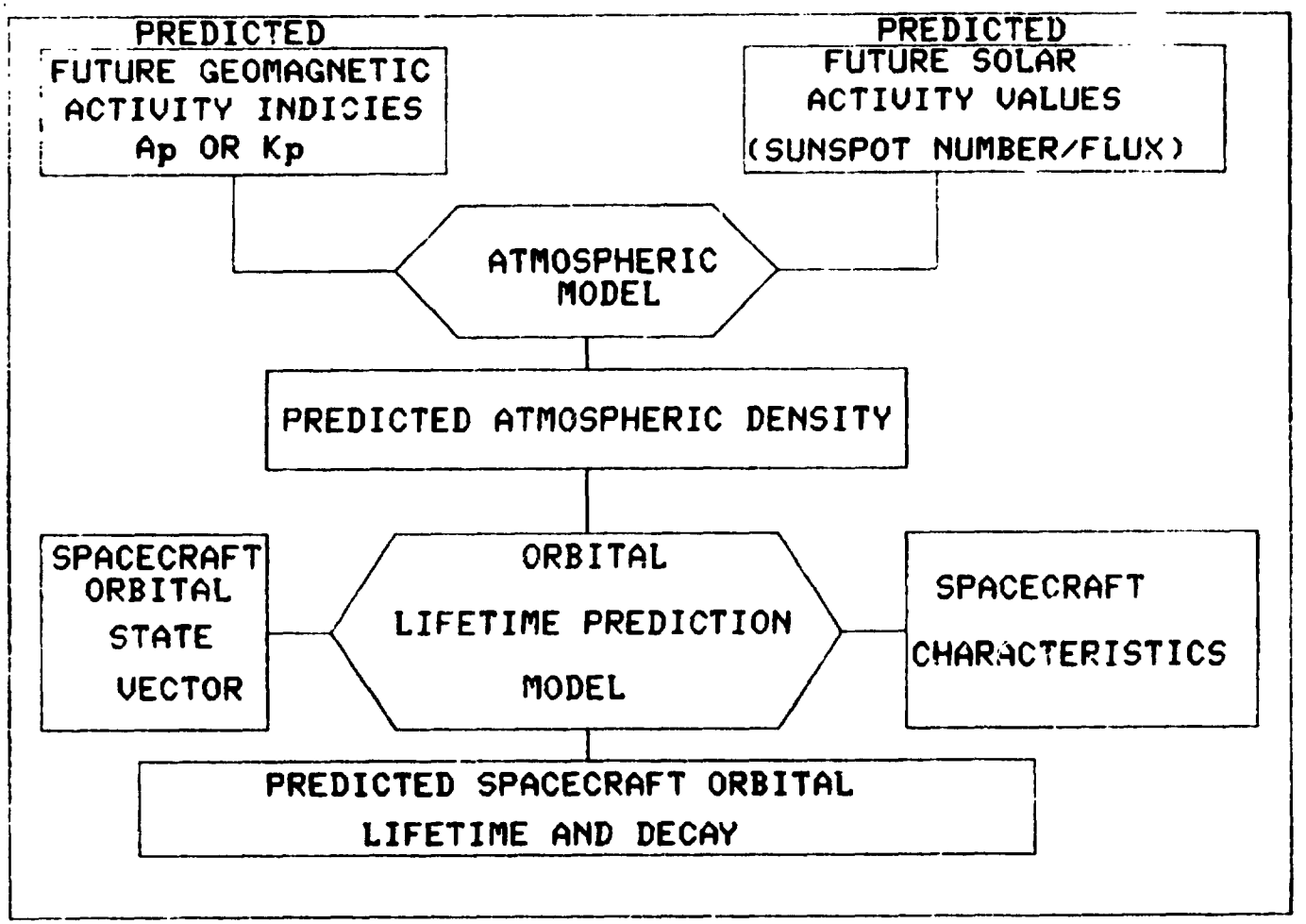

Figure 1.- Flow chart for predicted solar activity input values.

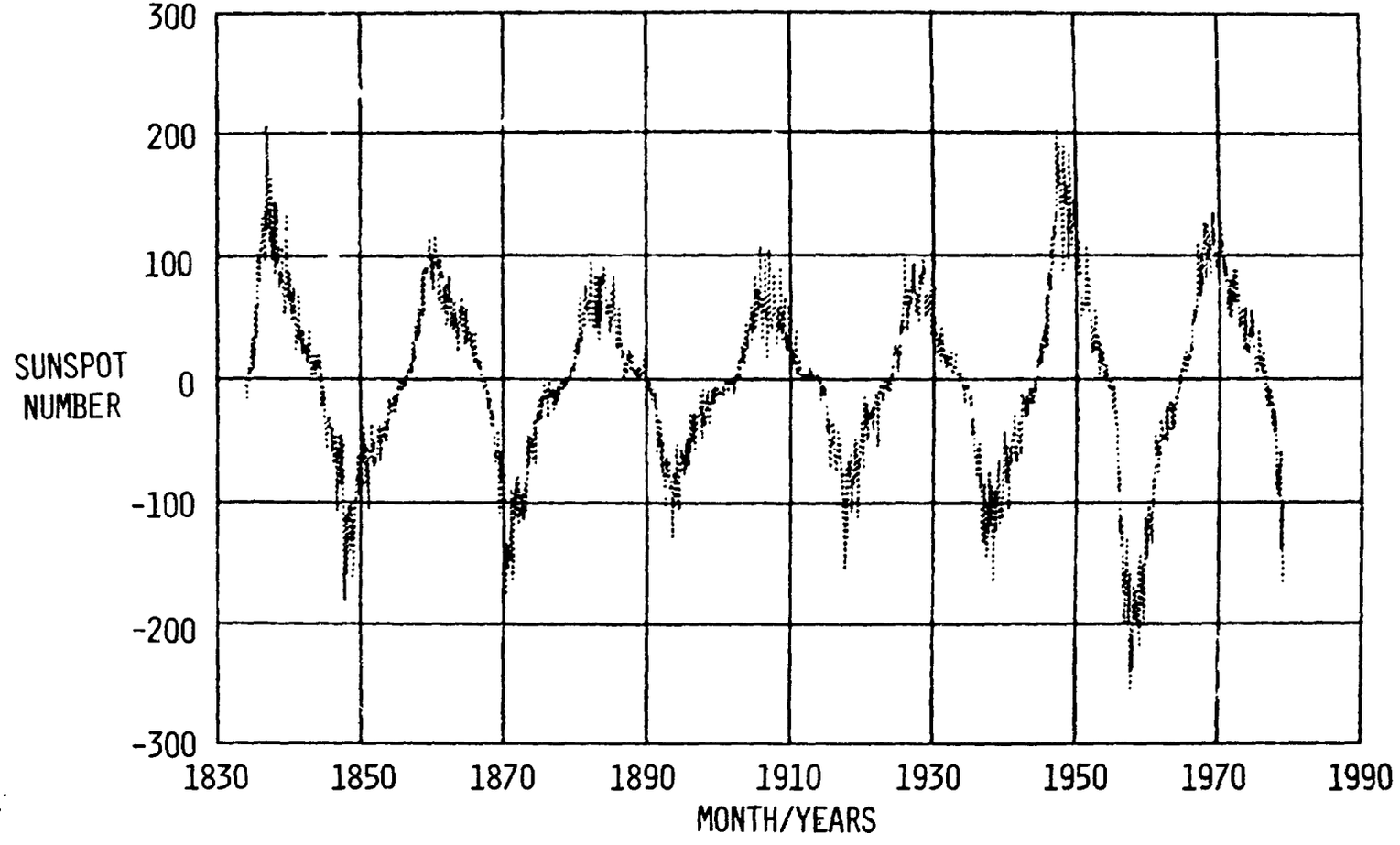

Figure 2.- Sunspot number solar cycles monthly mean values (1834-1979).

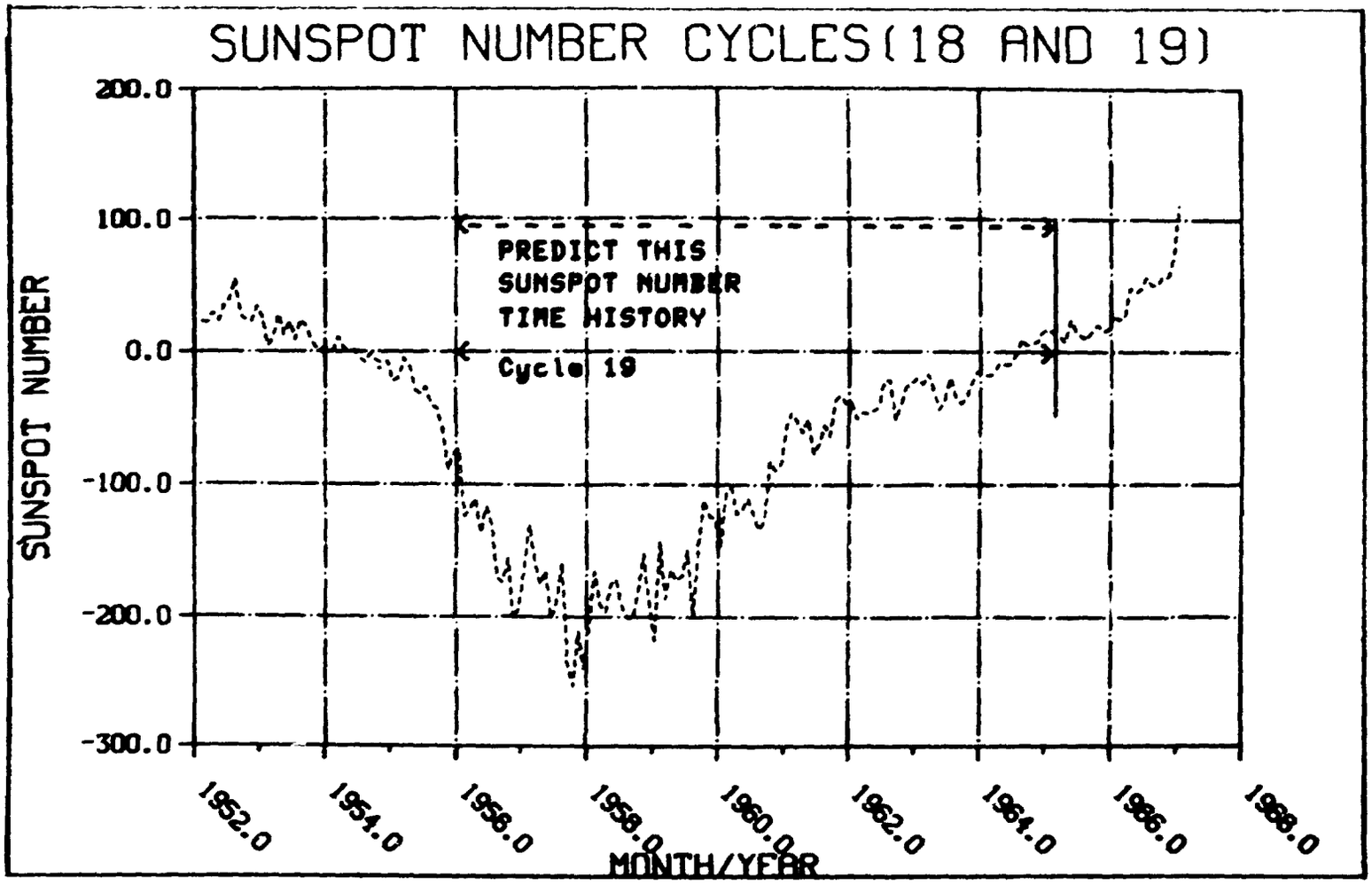

Figure 3.- Sunspot number time history of values to predict (1956-1965).

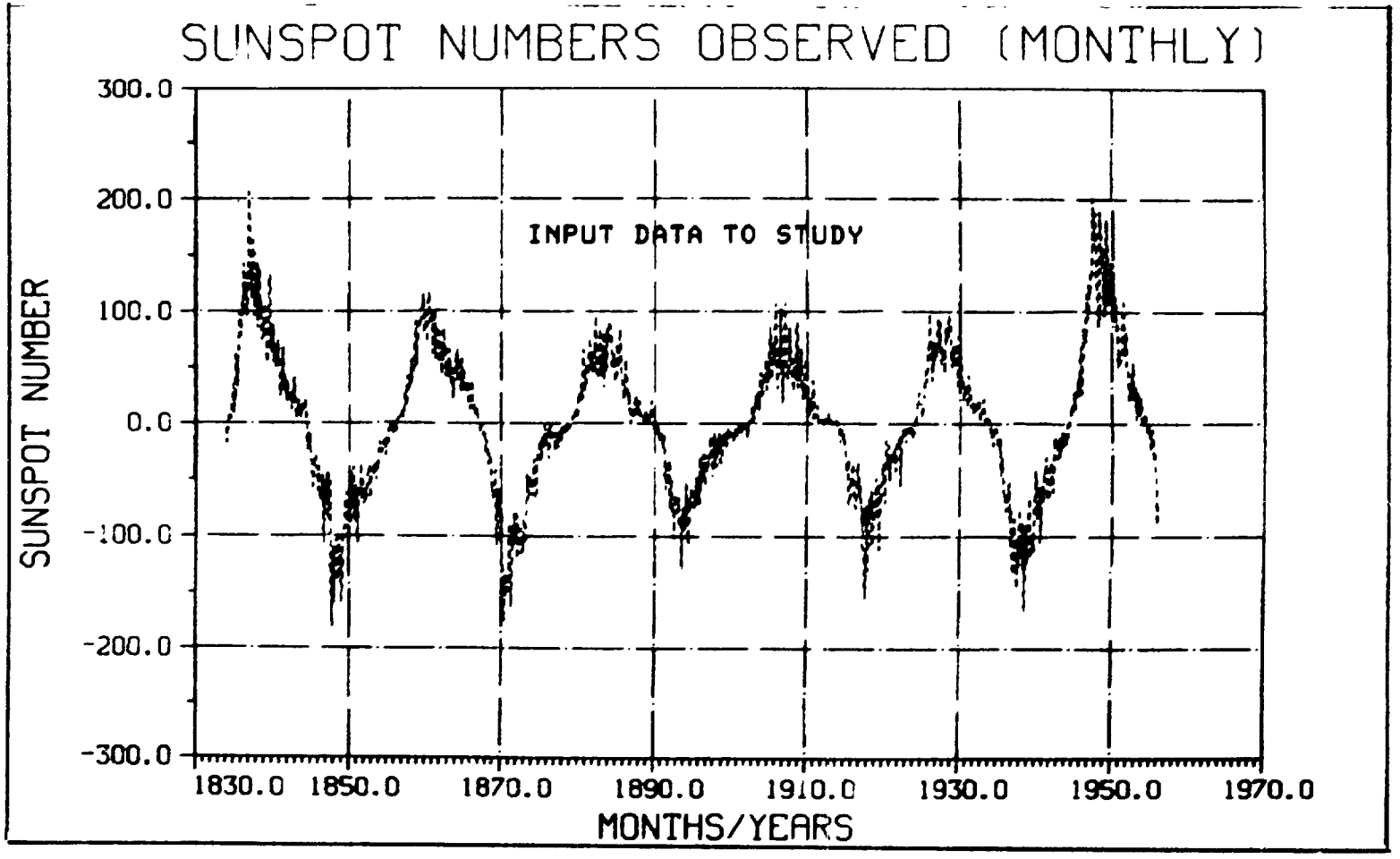

Figure 4.- Sunspot number record used as input to study (1830-January 1956).

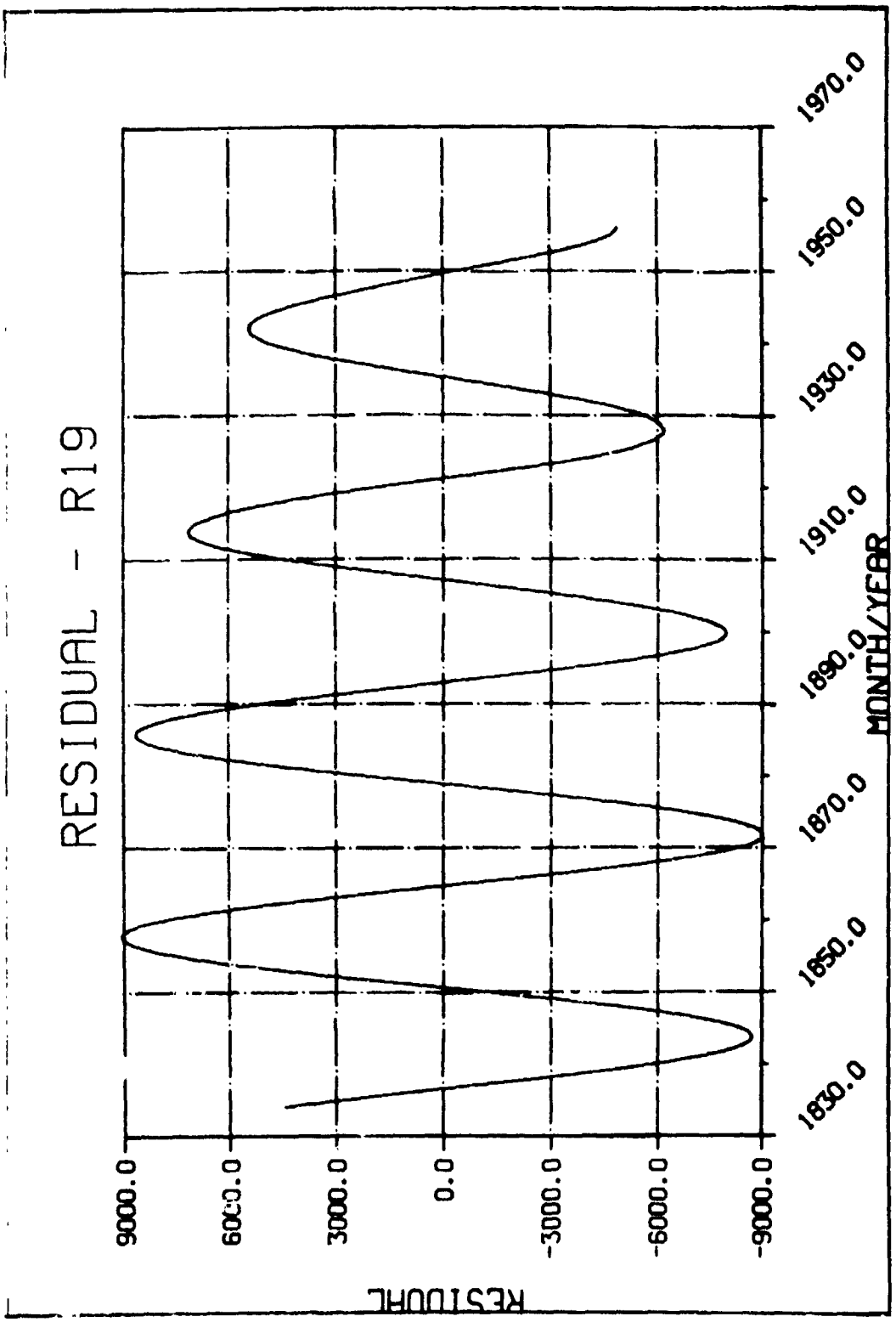

Figure 5.- Final residual curve R19 (1830-January 1956).

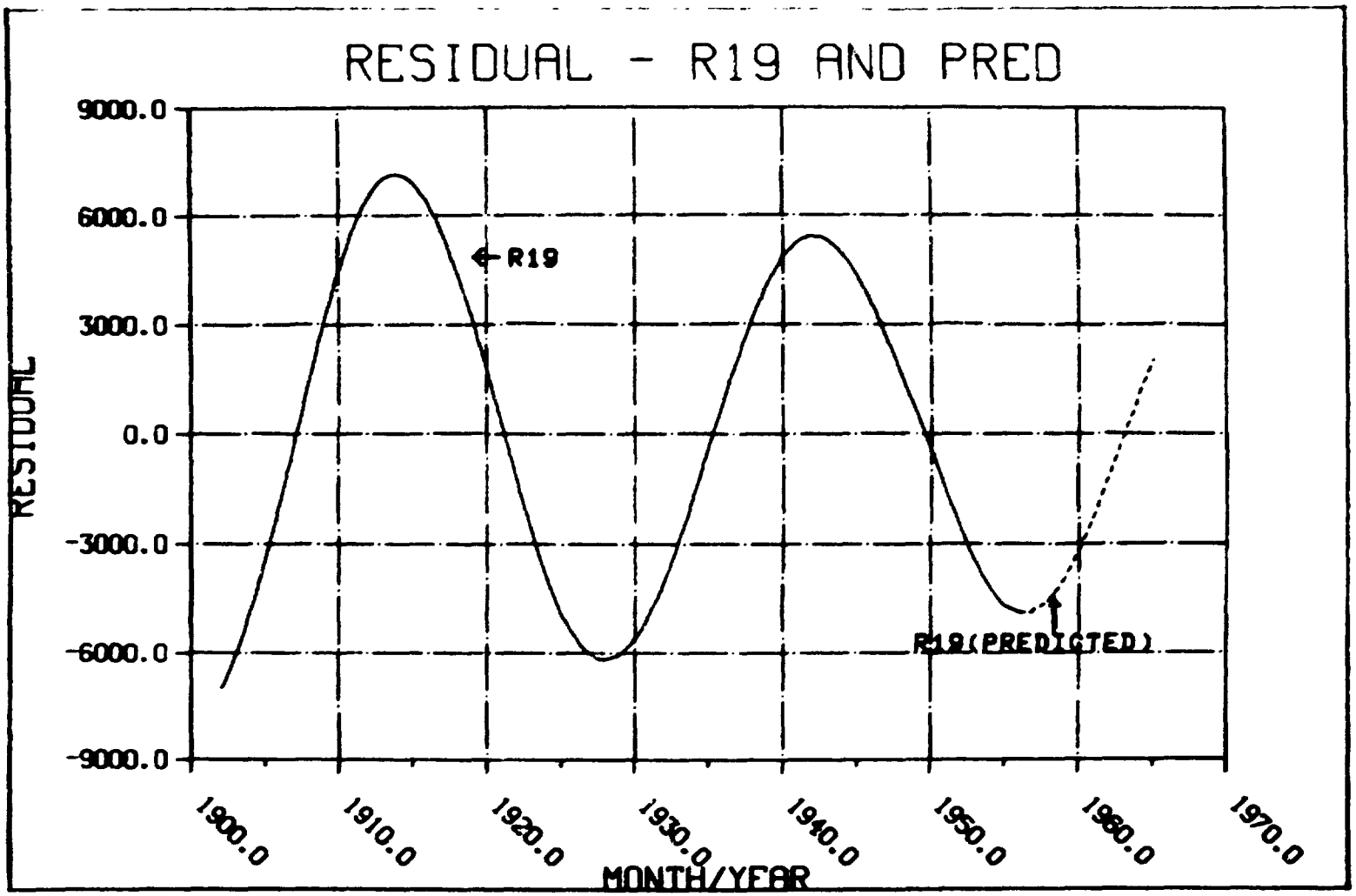

Figure 6.- Final residual and predicted residual curve R19.

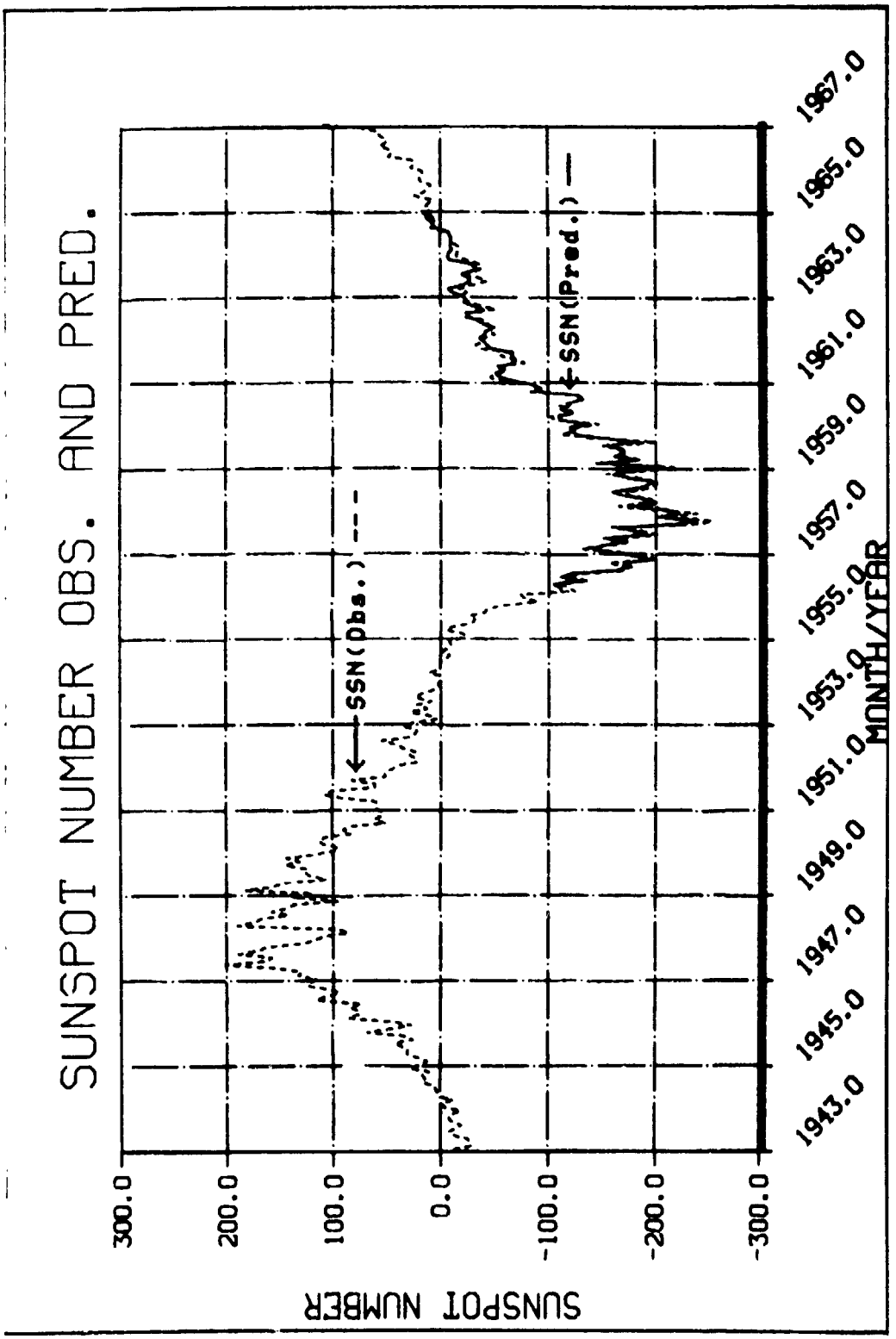

Figure 7.- Sunspot numbers (observed and predicted) (1943-January 1965).

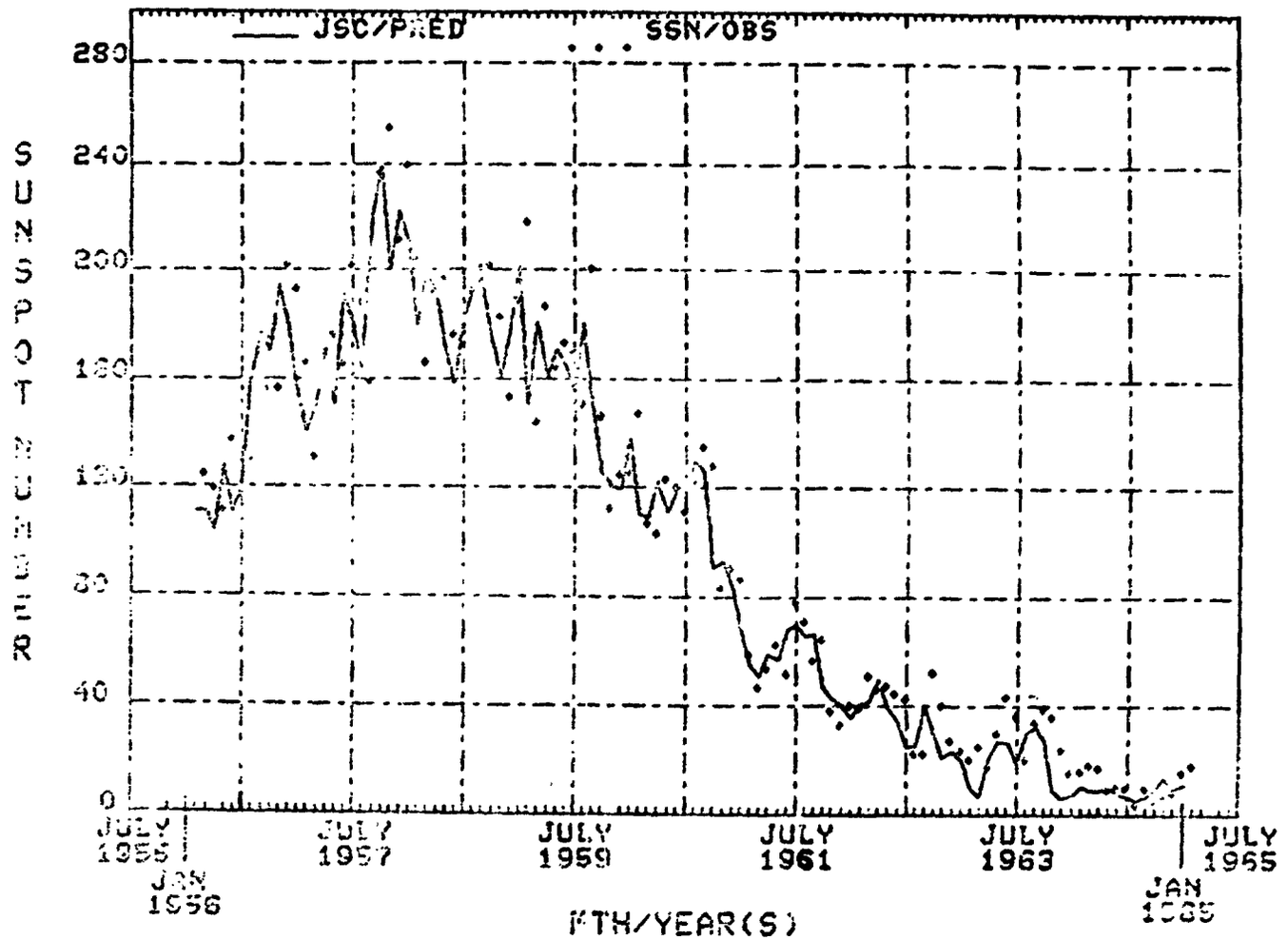

Figure 8.- Final predicted and observed sunspot numbers (January 1956-January 1965).

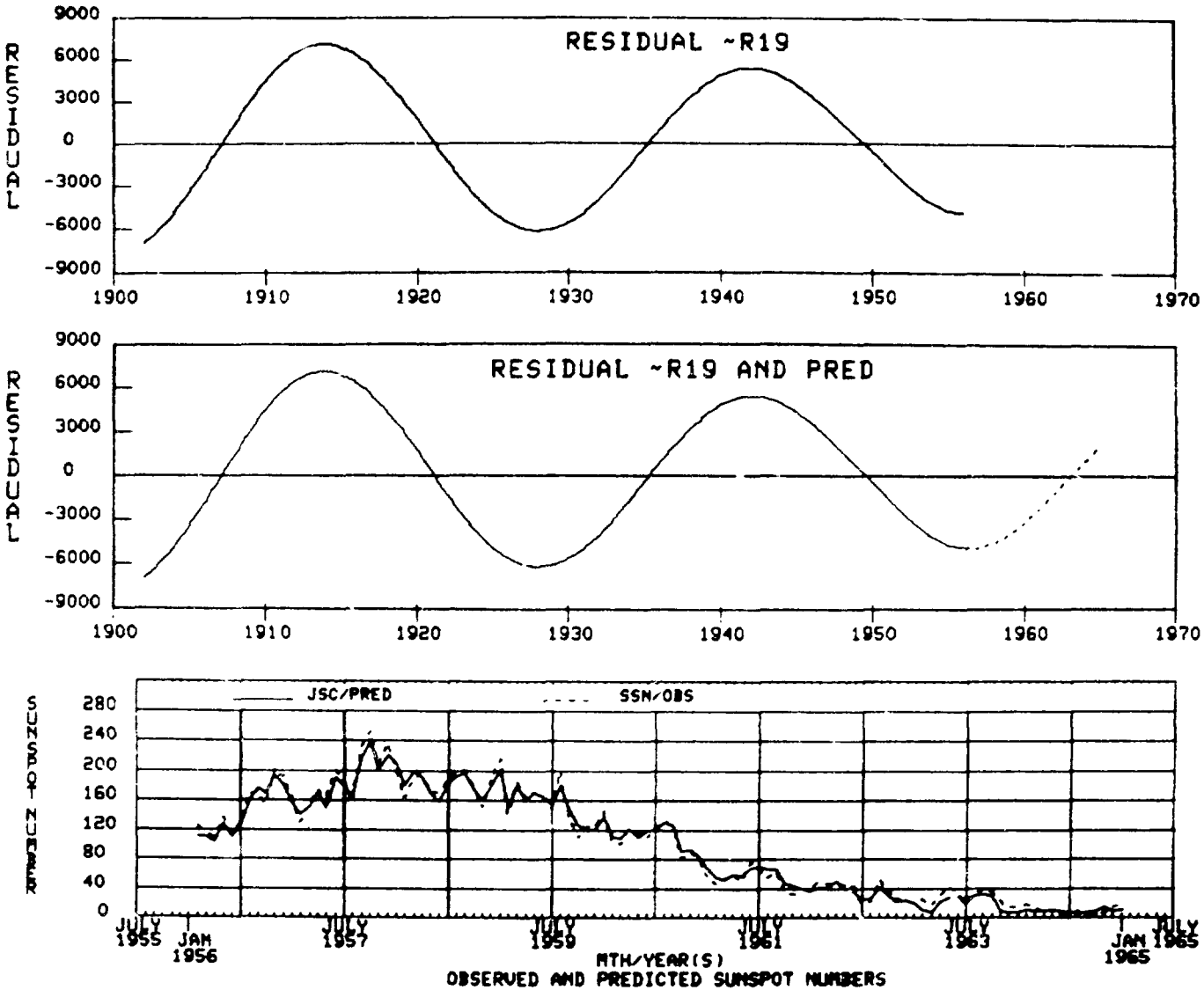

Figure 9.- Final summary plot R19 study.

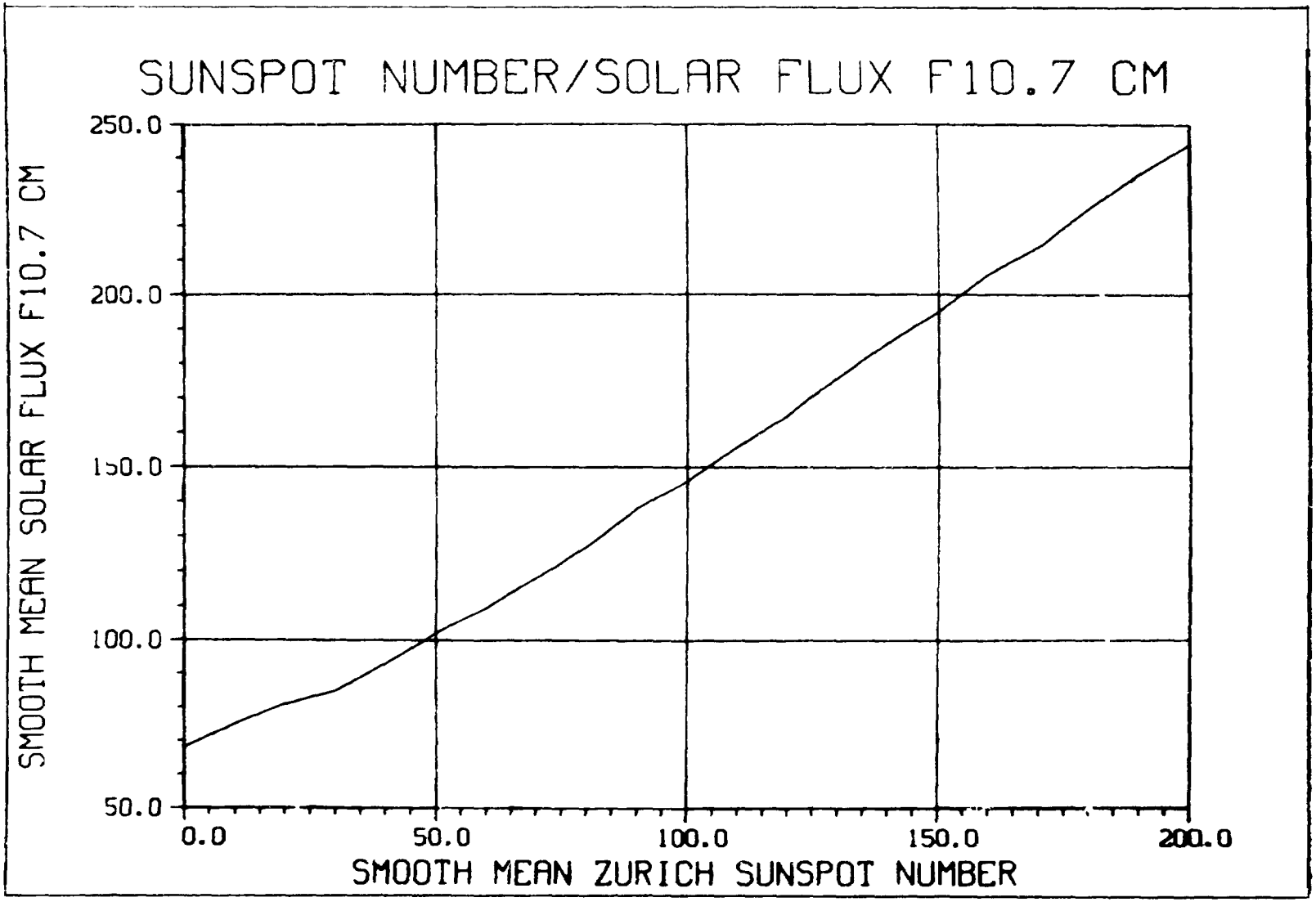

Figure 10.- Sunspot number/solar flux F10.7-cm model.

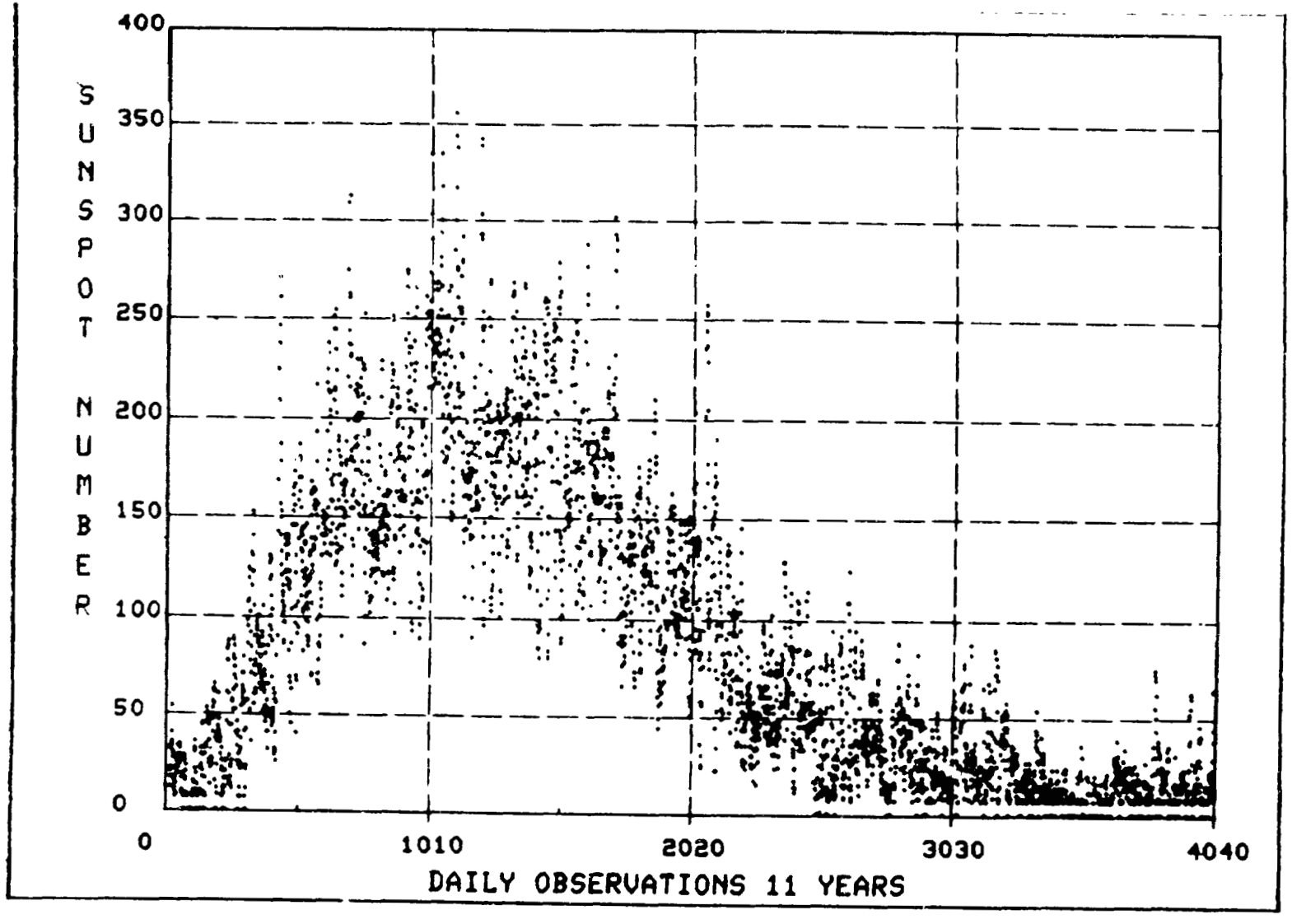

Figure 11.- Sunspot number daily observations (1955-1965).

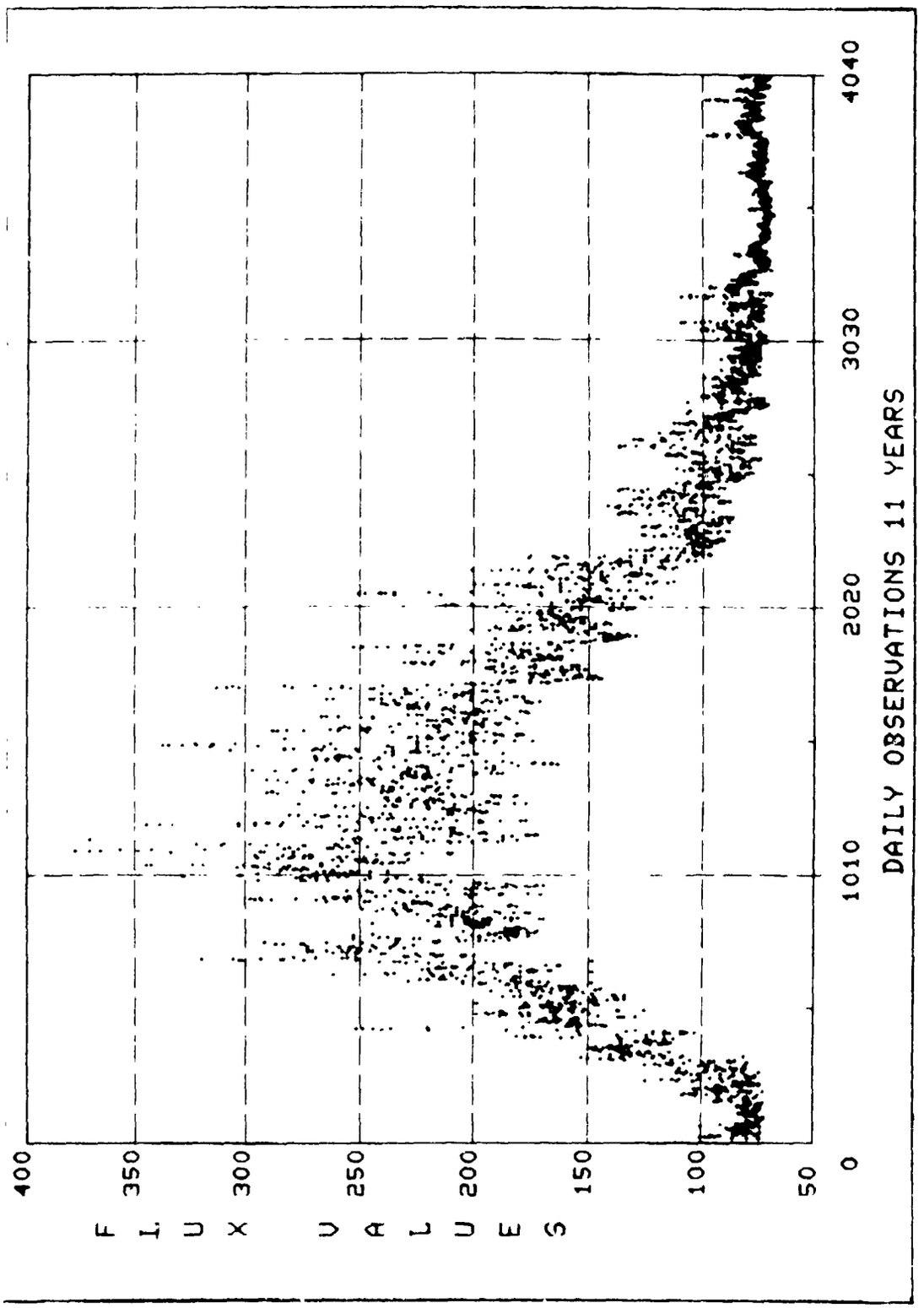

Figure 12.- Solar flux daily observations (1955-1965).

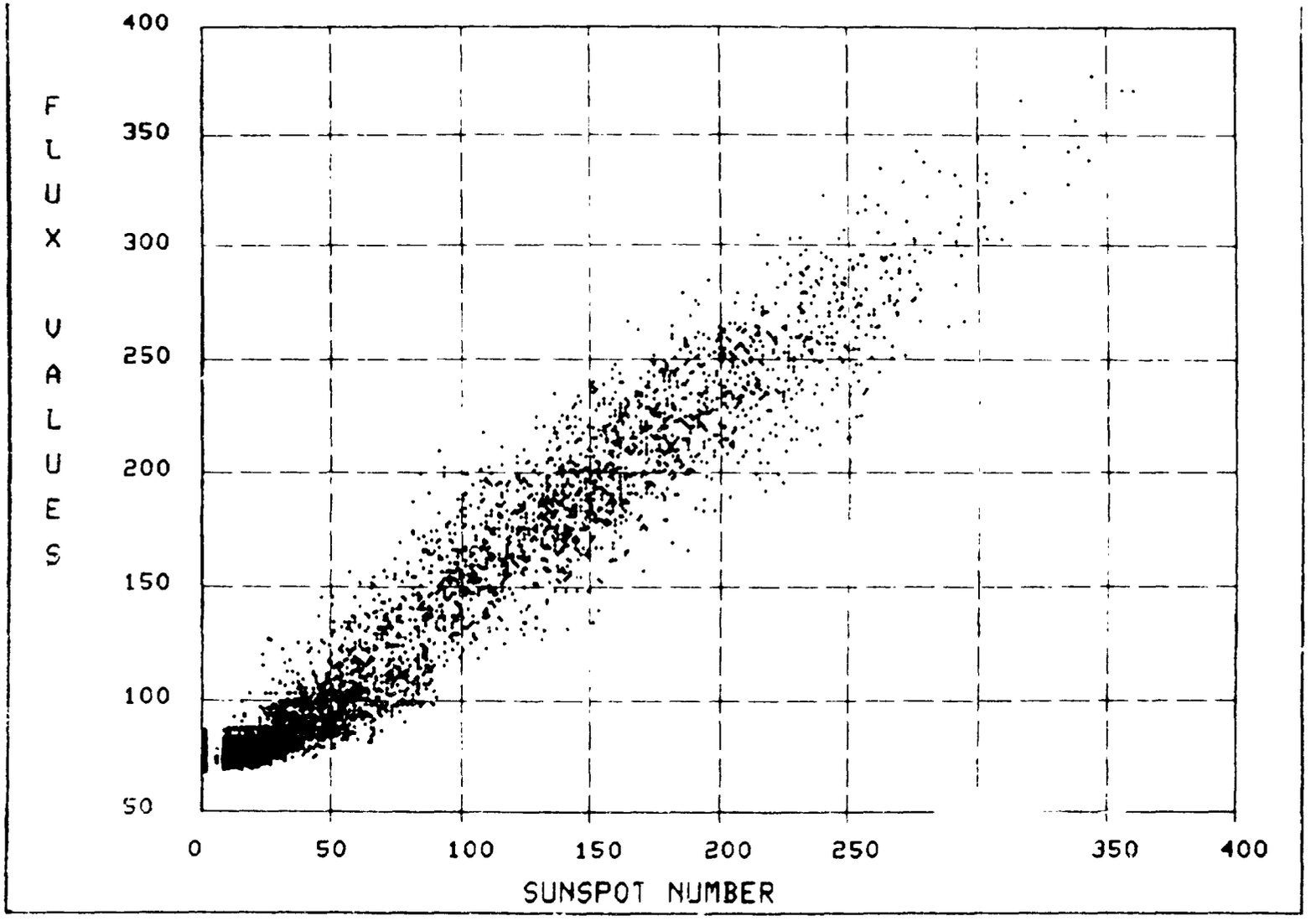

Figure 13.- Solar flux as a function of sunspot numbers for all samples.

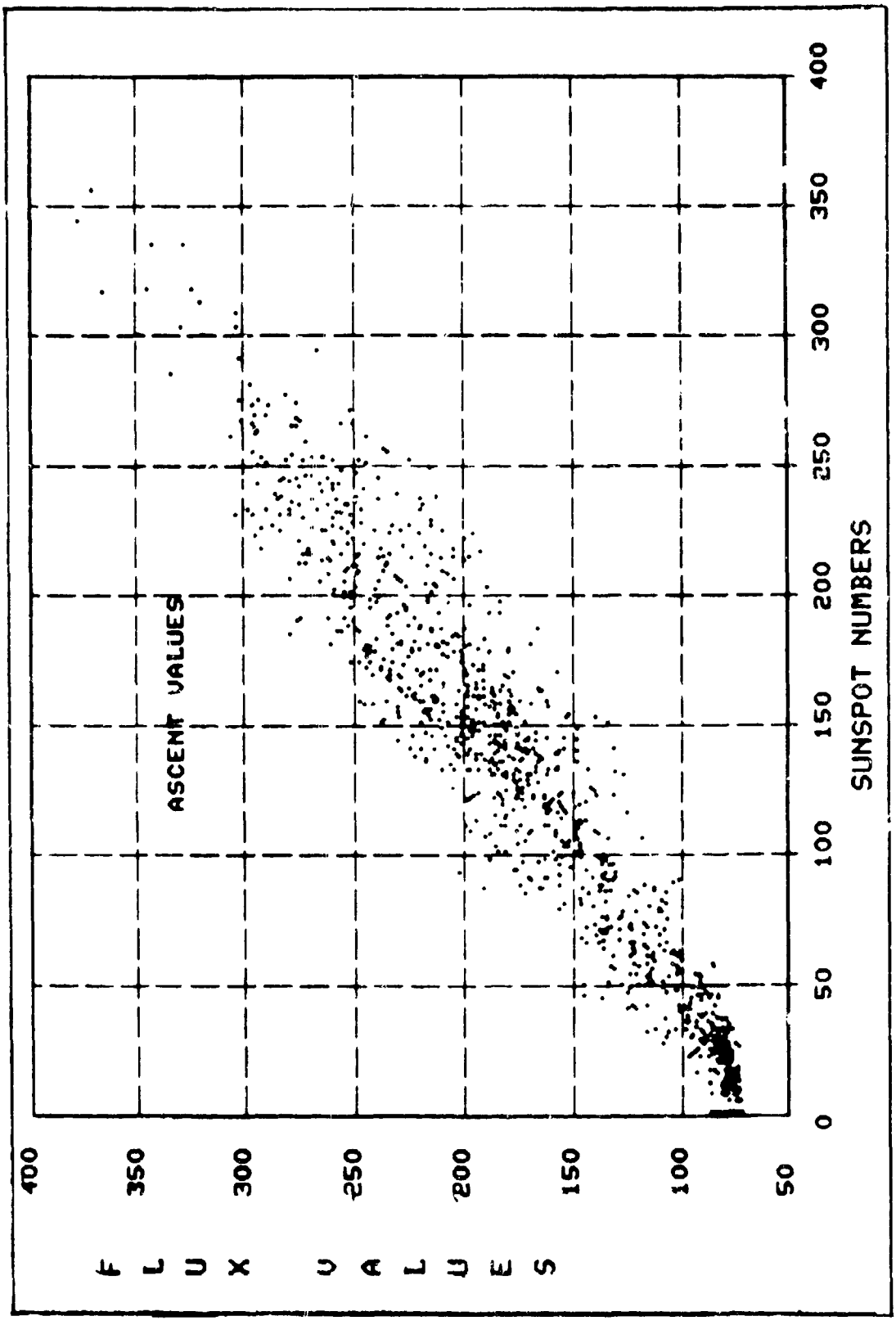

Figure 14.- Ascent solar flux as a function of sunspot numbers.

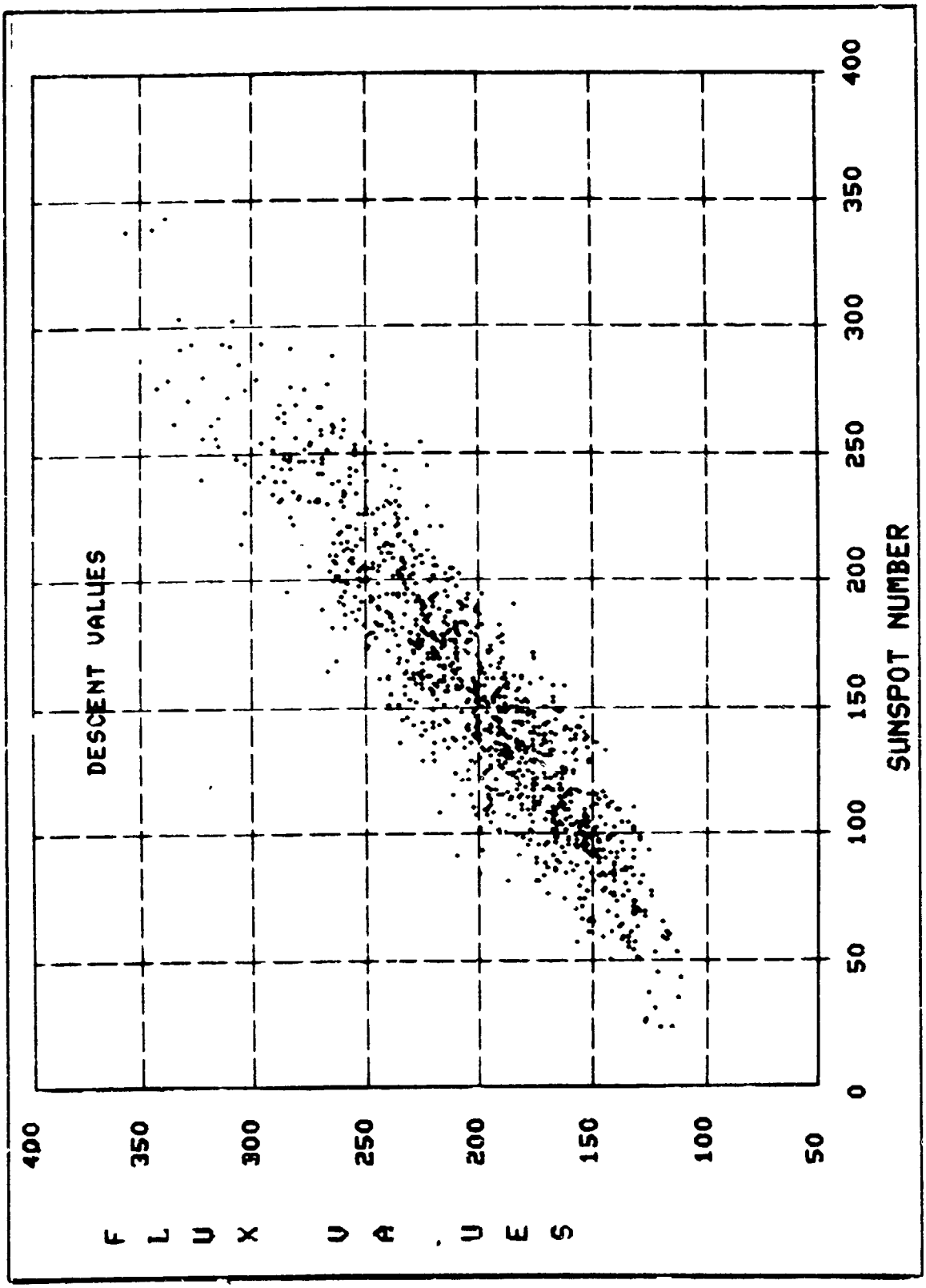

Figure 15.- Descent solar flux as a function of sunspot numbers.

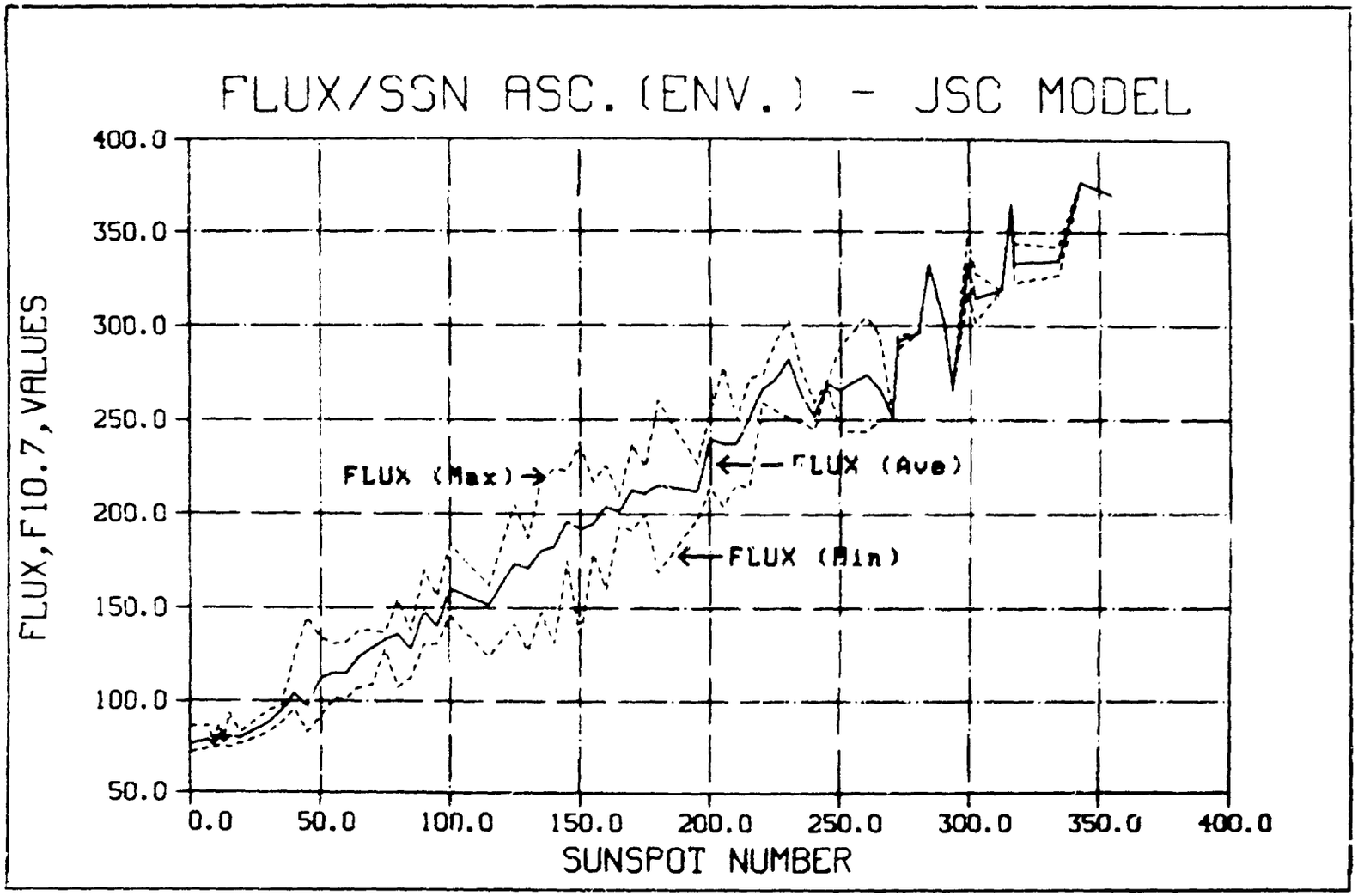

Figure 16.- JSC ascent flux/sunspot number envelope model.

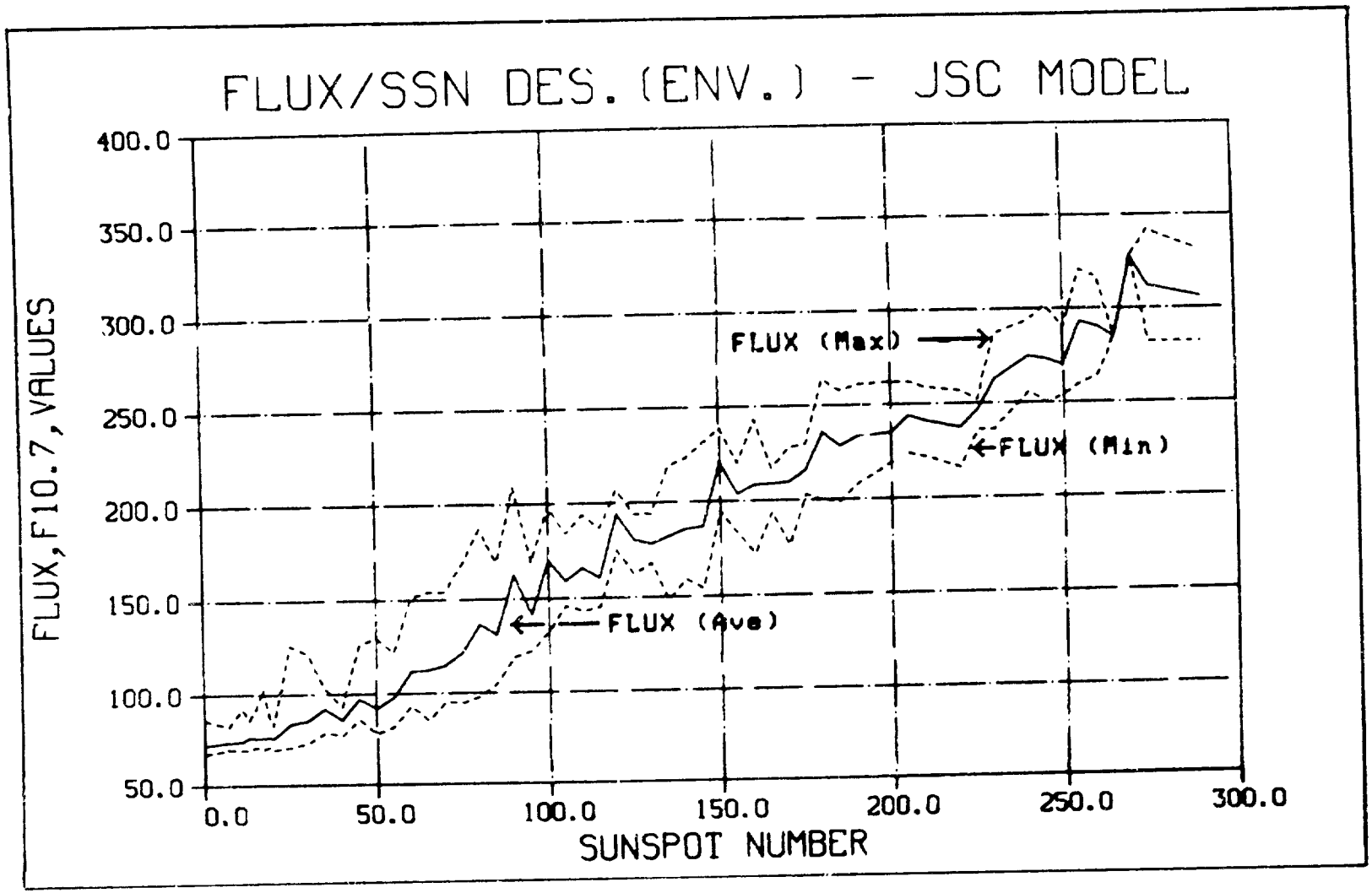

Figure 17.- JSC descent flux/sunspot number envelope model.

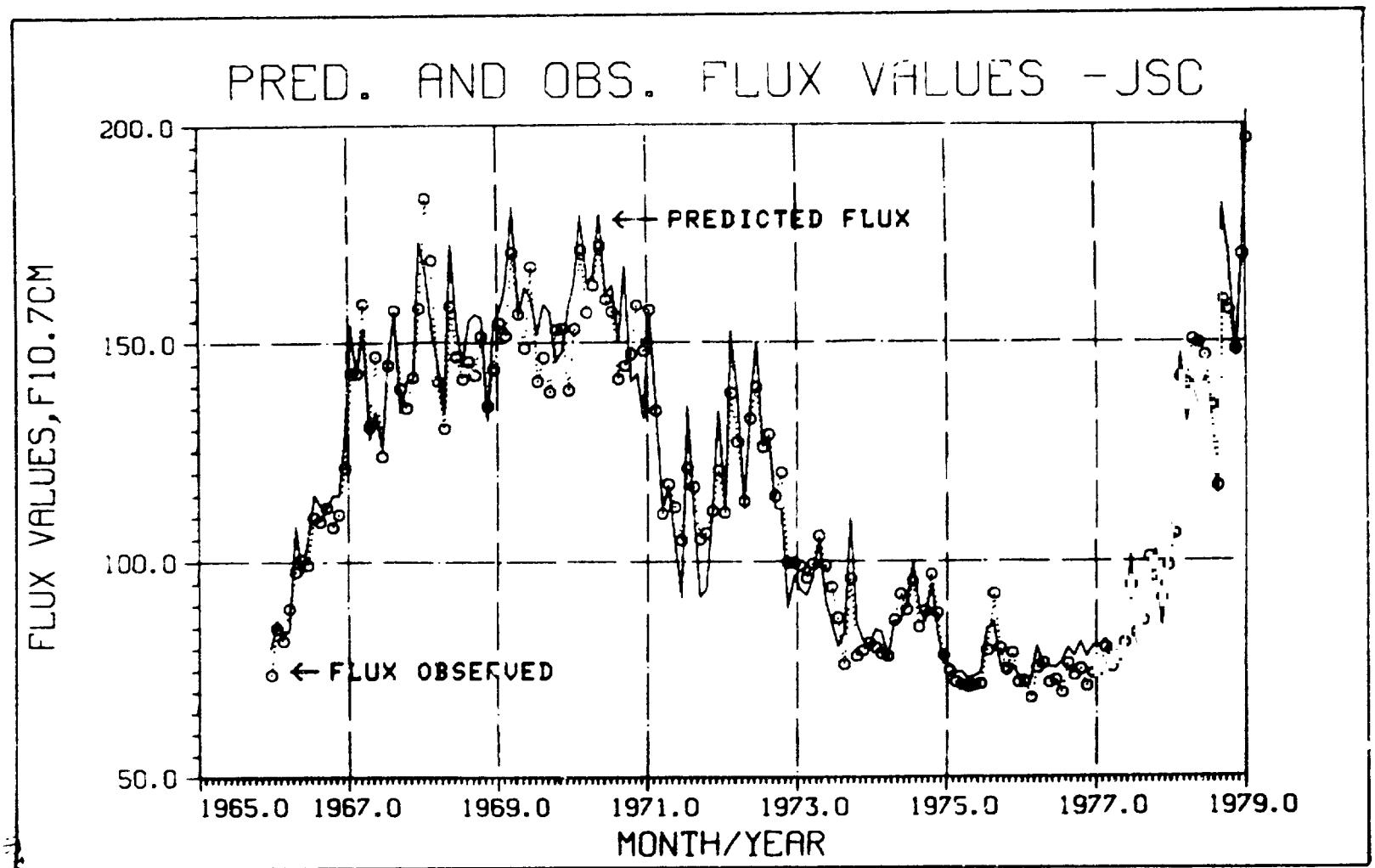

Figure 18.- Predicted and observed solar flux values (1965-1979).

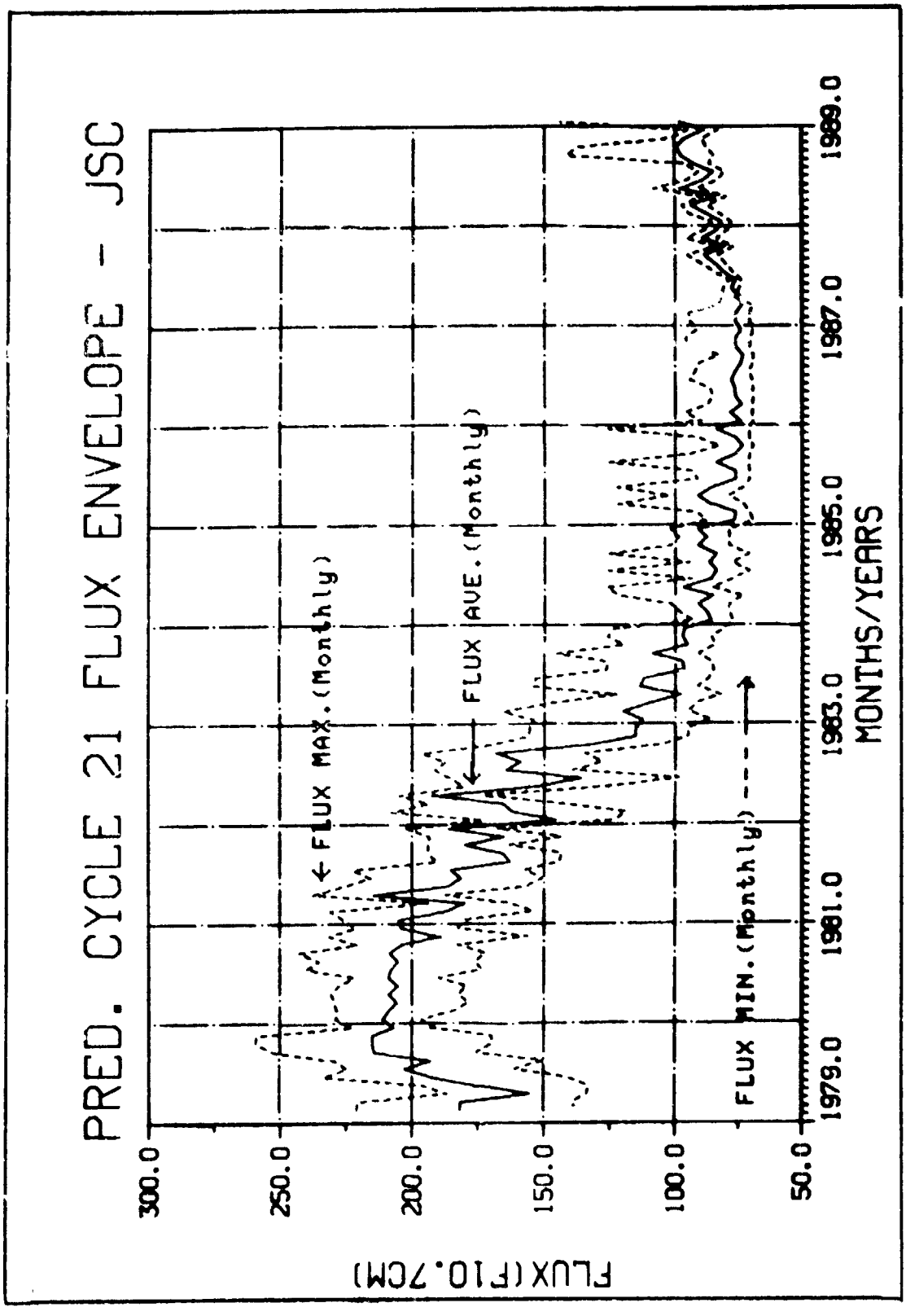

Figure 19.- JSC predicted monthly solar flux envelope (1979-1989).

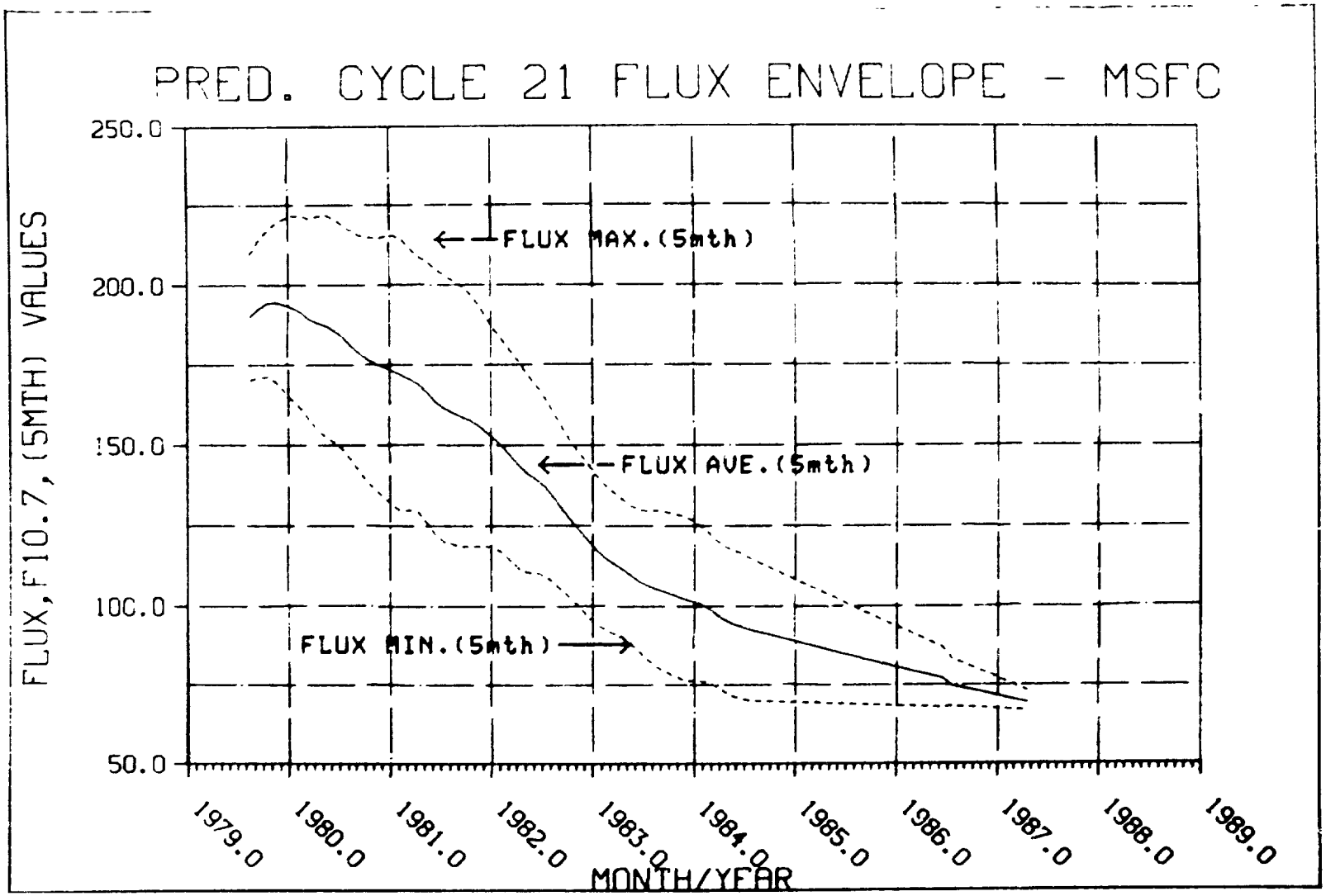

Figure 20.- MSFC predicted 5-month smooth solar flux envelope (1979-1987).

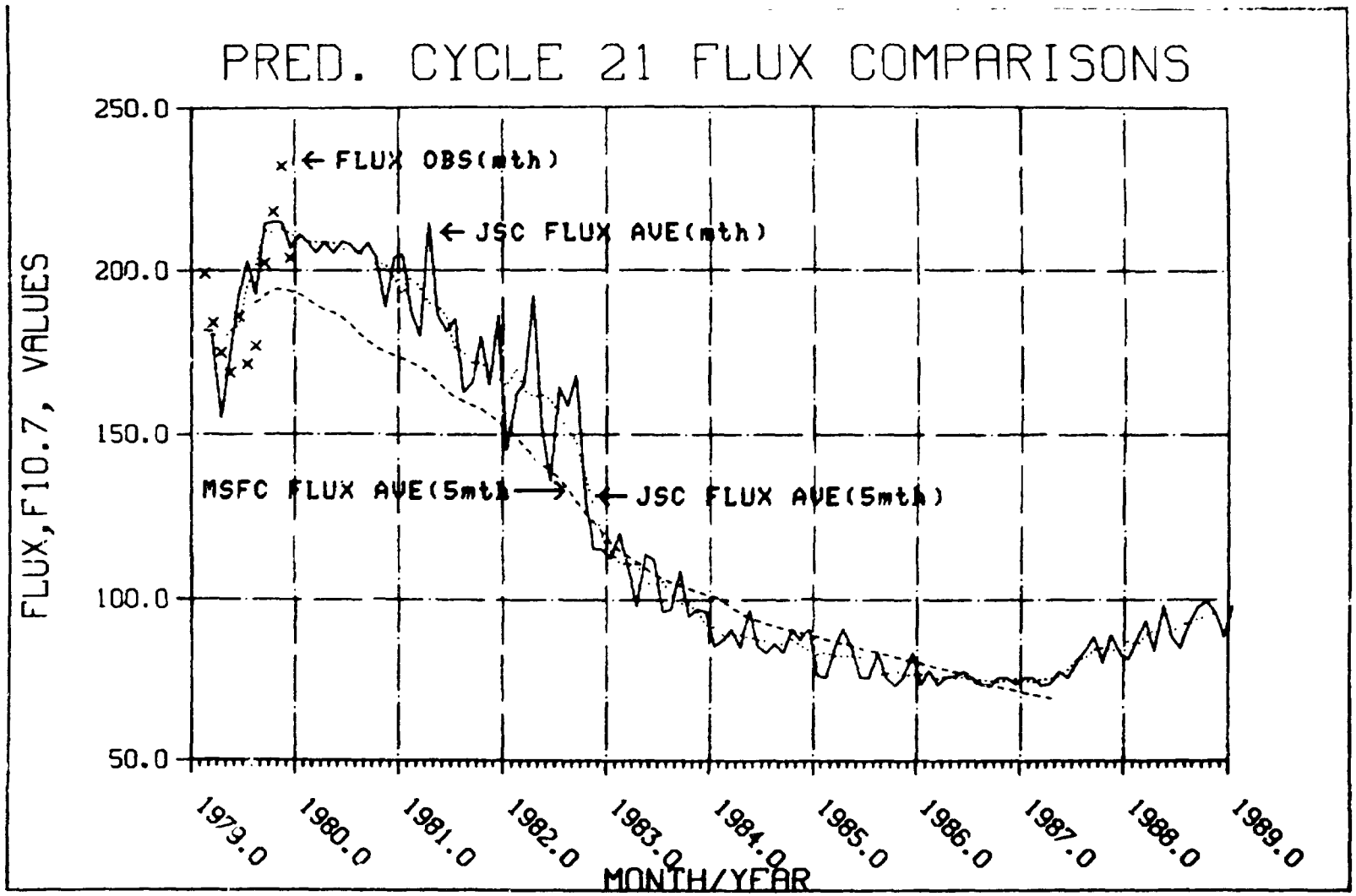

Figure 21.- JSC and MSFC predicted solar flux values including monthly observed flux.

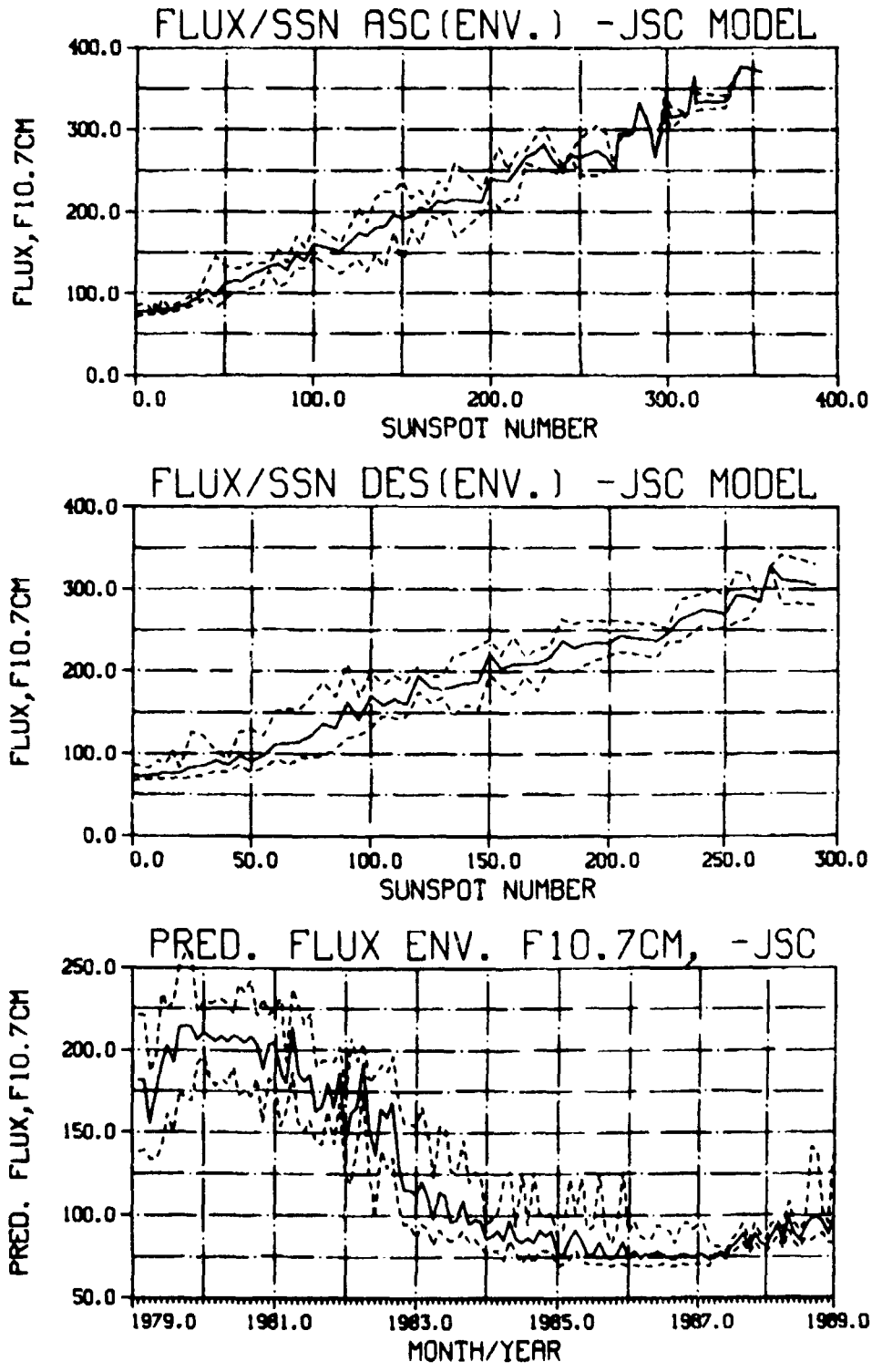

Figure 22.- Predicted solar flux envelope with the JSC sunspot number/flux models.

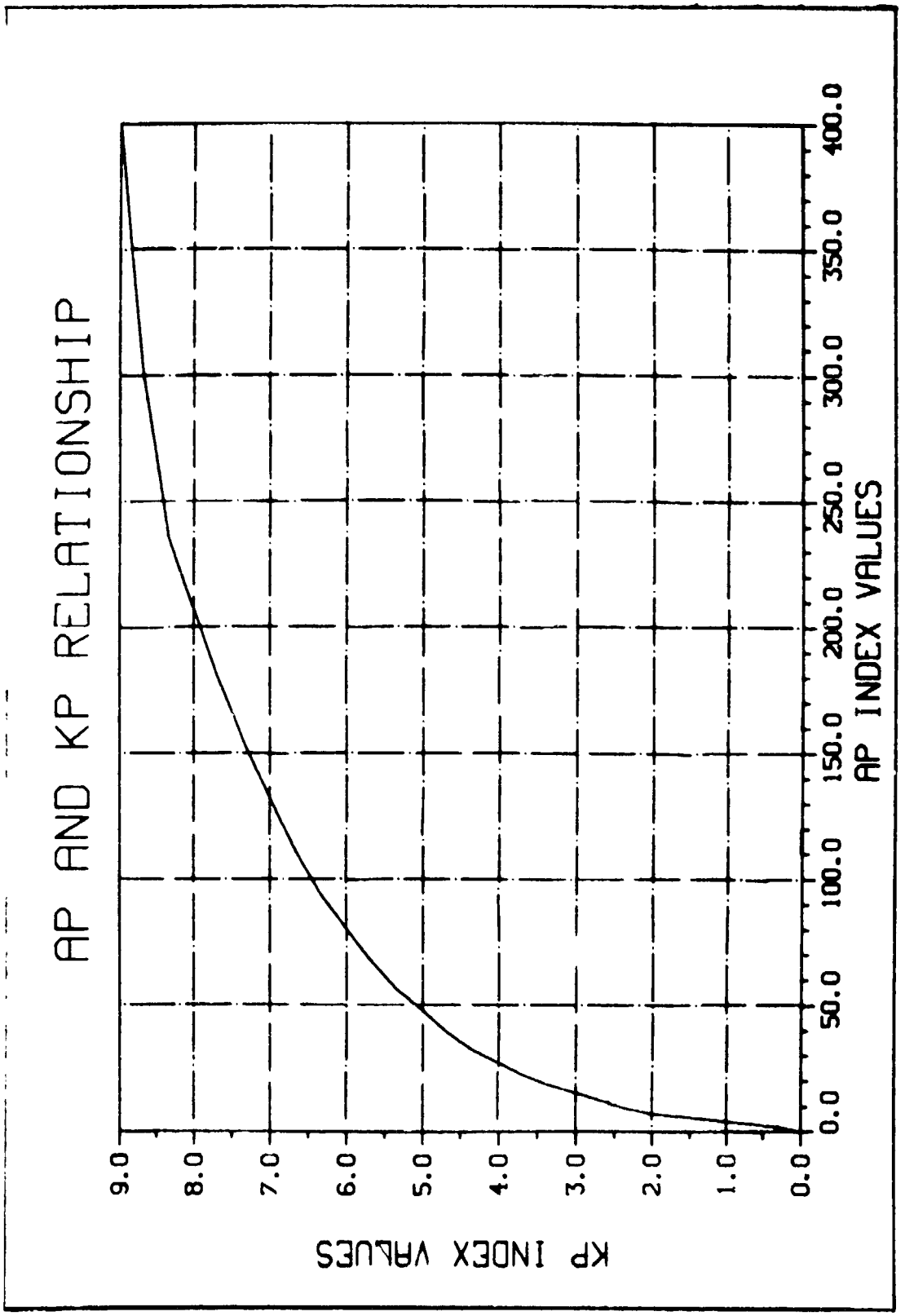

Figure 23.- Geomagnetic indices A_p and K_p relationship.

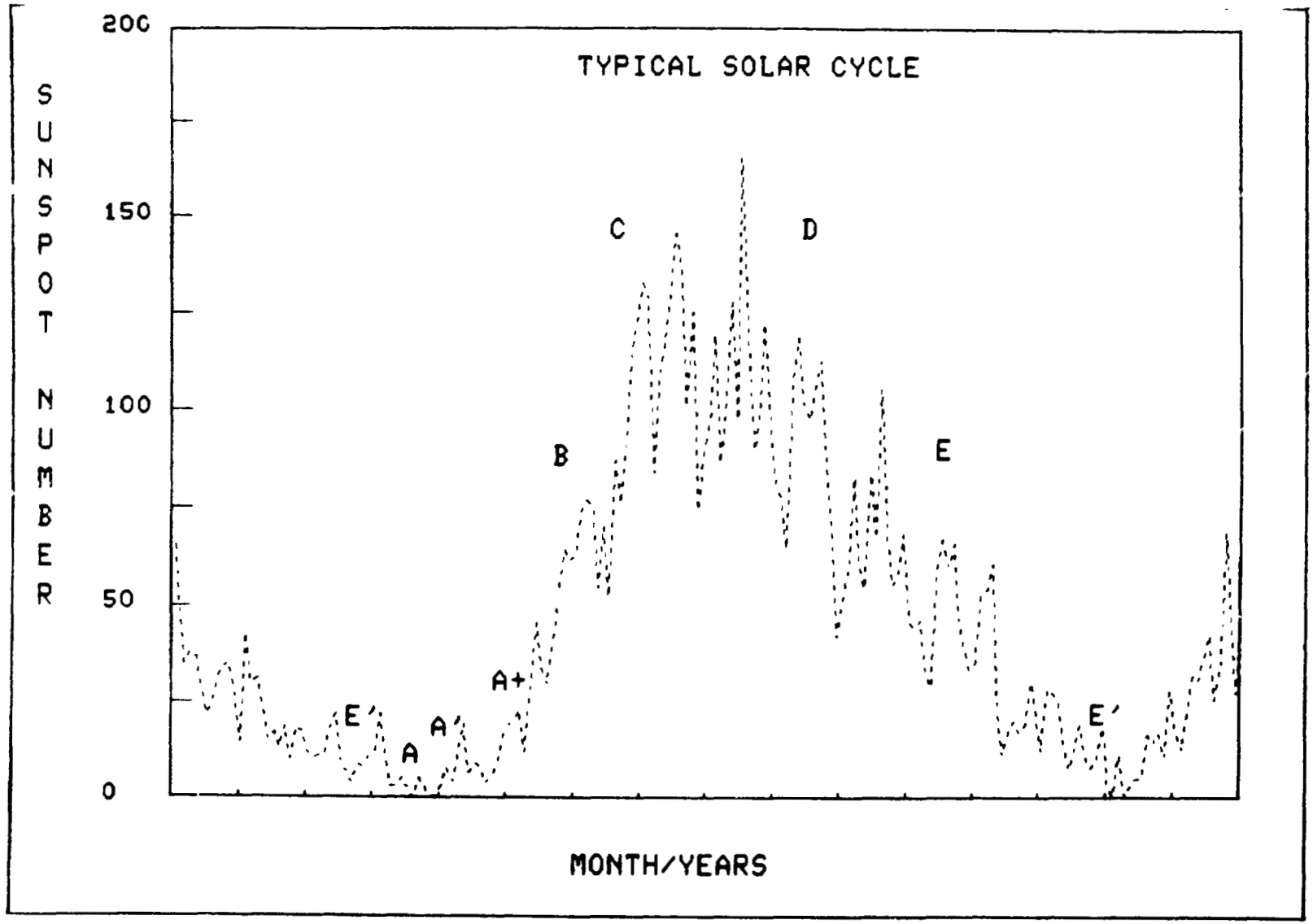

Figure 24.- Classification of the solar cycle for the geomagnetic index A_p models.

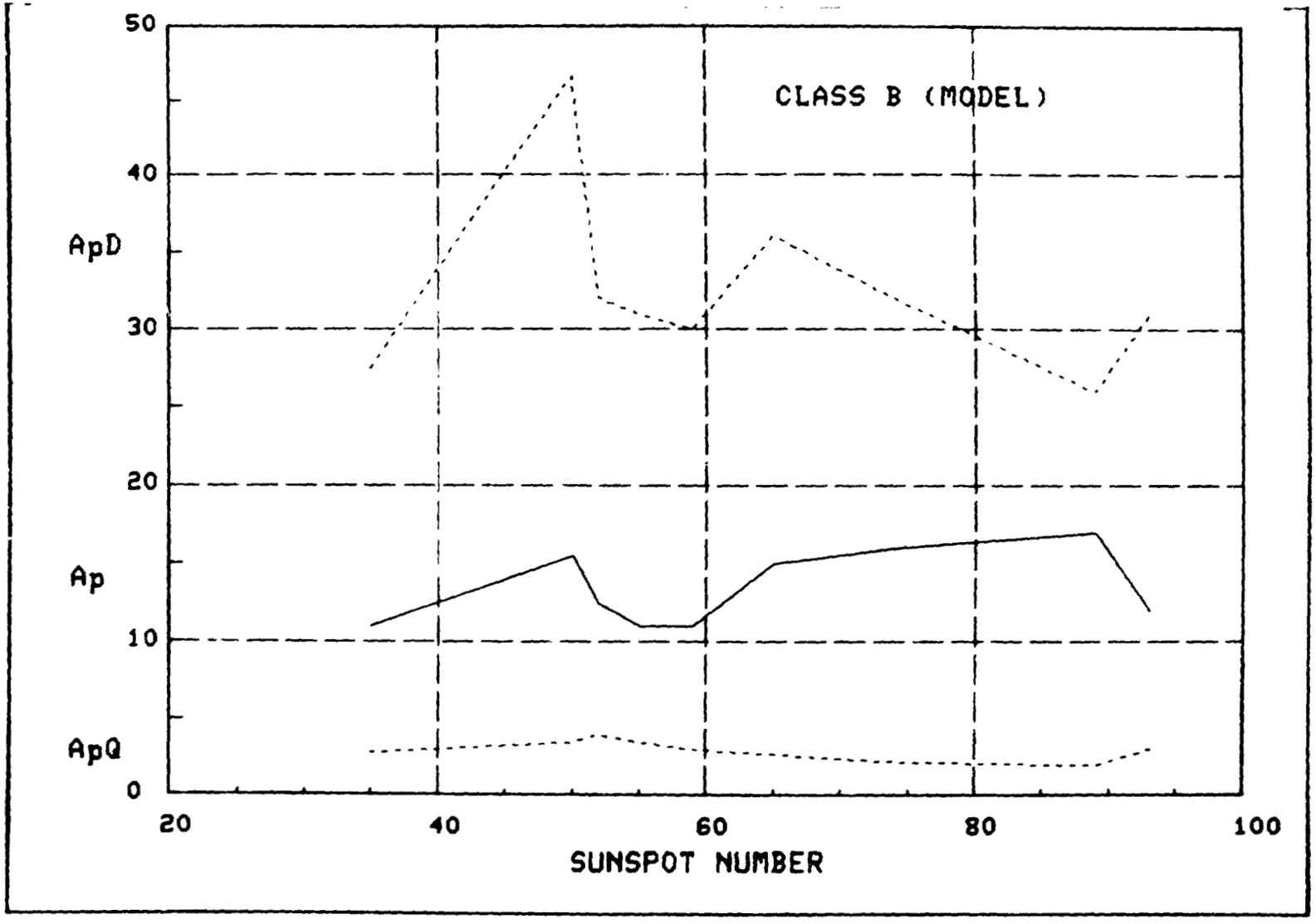

Figure 25.- The geomagnetic indices class B(model), mean A_pD, A_p, and A_pQ values as a function of sunspot number.

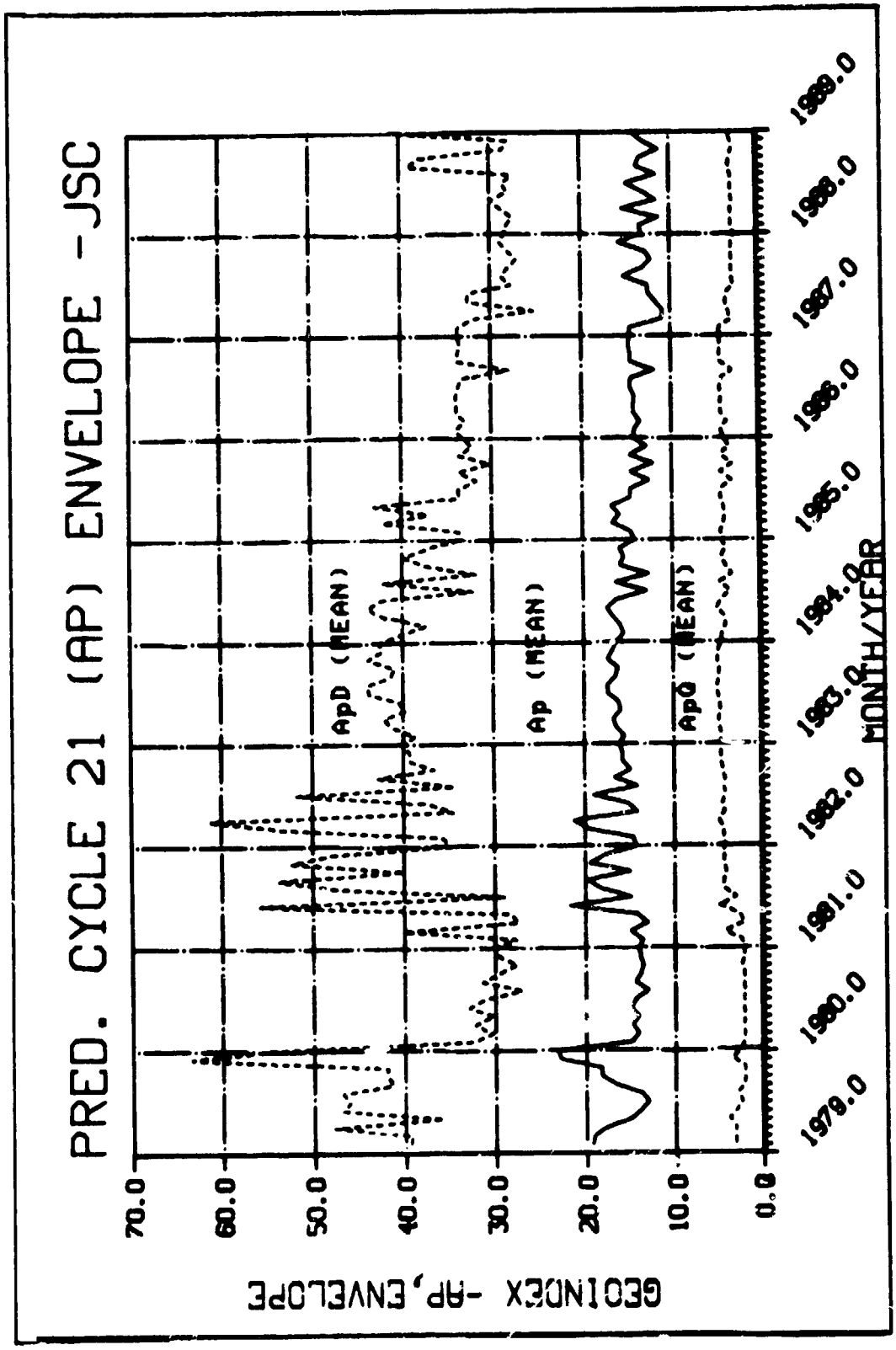

Figure 26.- JSC predicted envelope of the mean geomagnetic indices (A_pD, A_p, A_pQ) for (1979-1989).

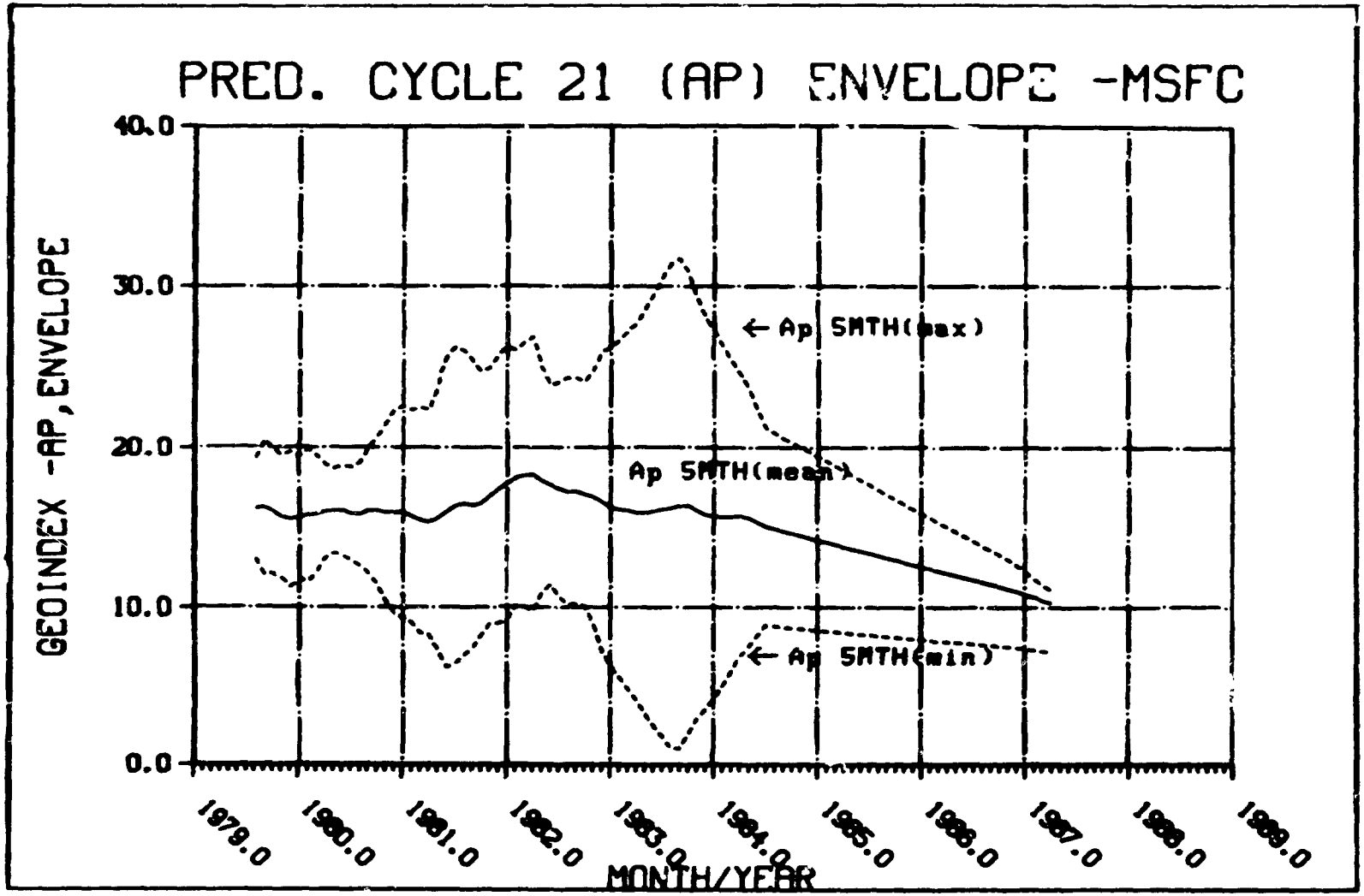

Figure 27.- MSFC predicted envelope of the 5-month smooth geomagnetic index A_p (1979-1987).

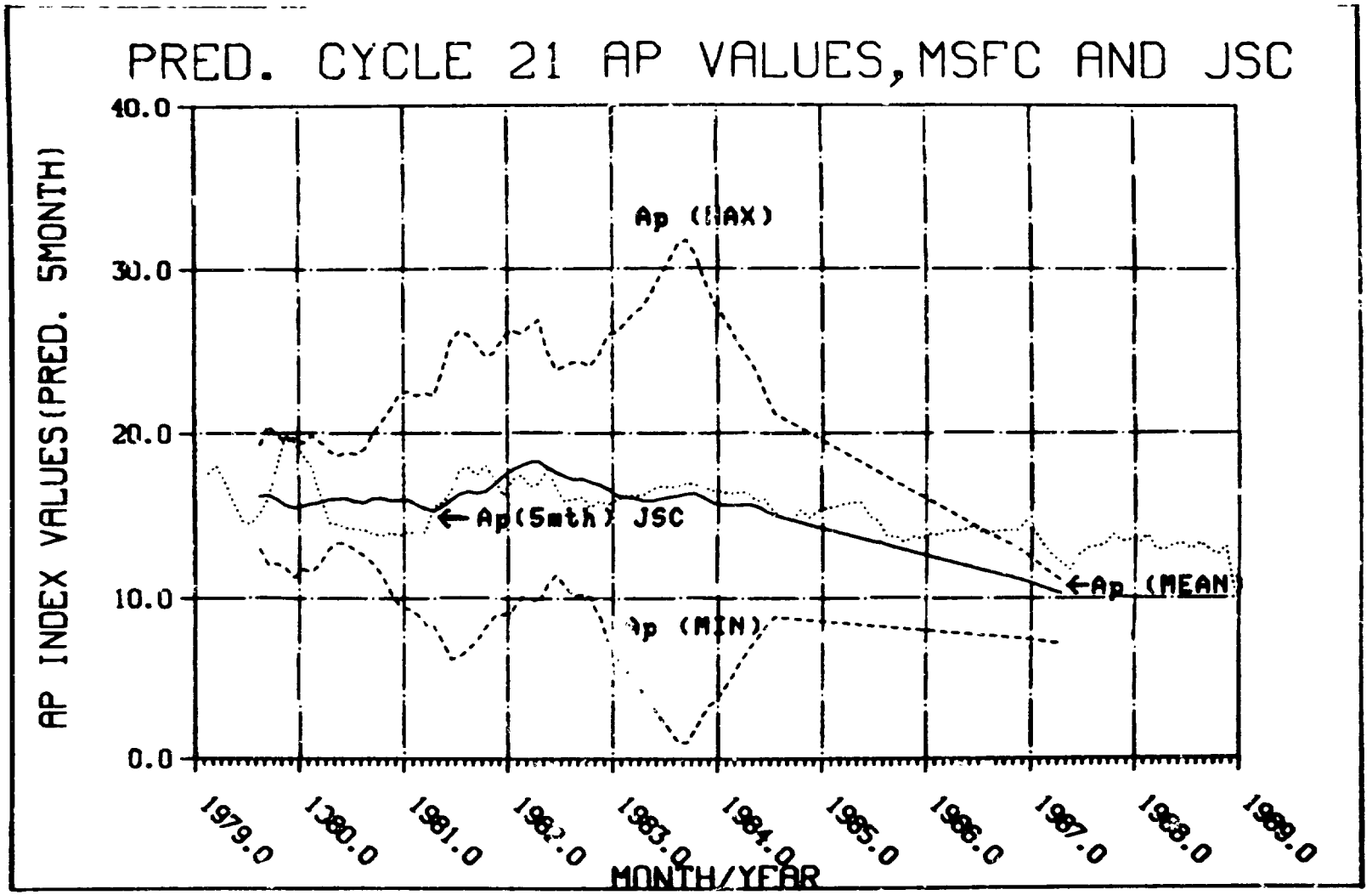

Figure 28.- Comparison of the JSC 5-month smooth A_p predicted index with the MSFC predicted 5-month smooth A_p envelope.

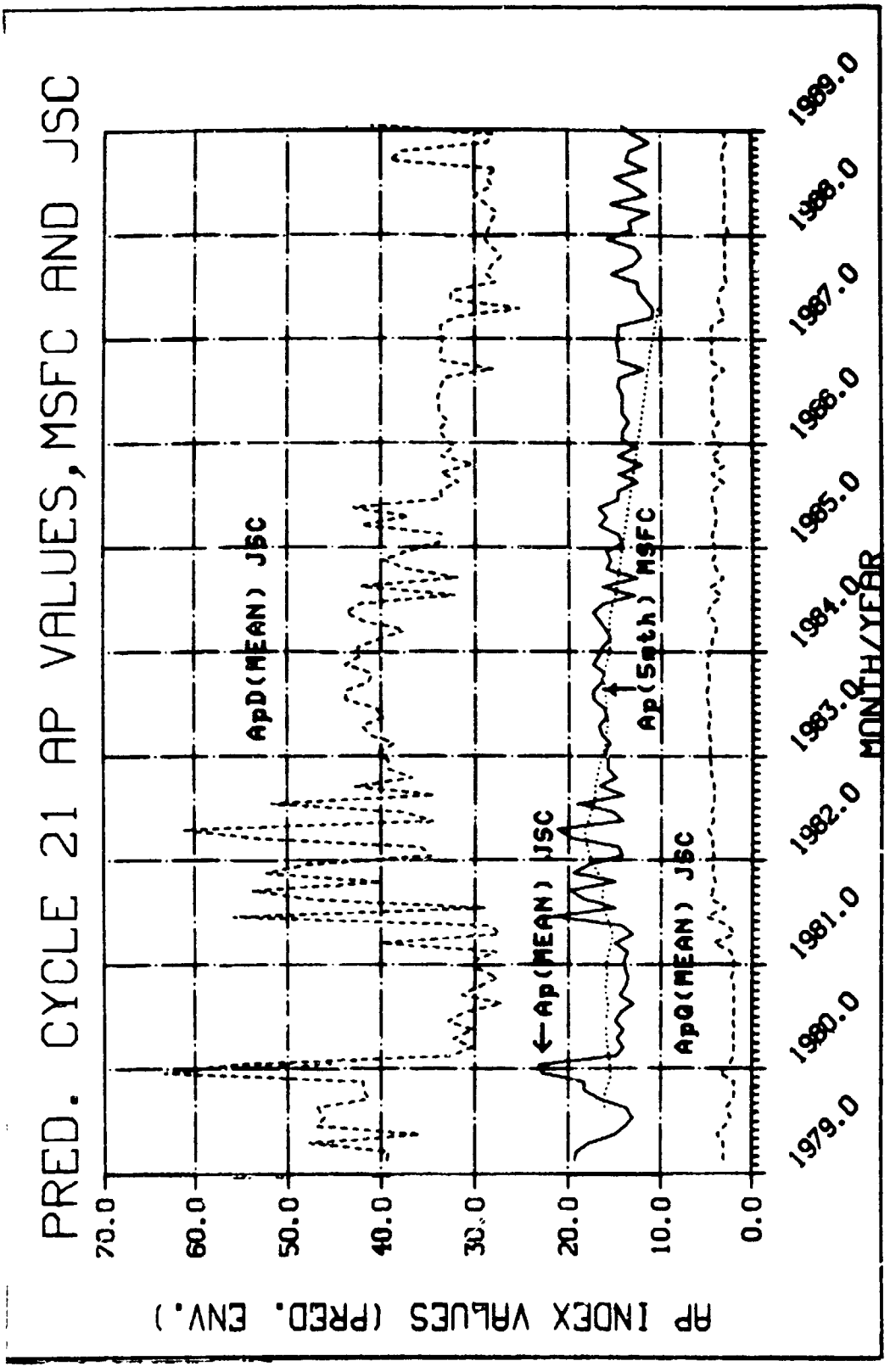

Figure 29.- Comparison of the MSFC 5-month smooth A_p predict. index with the JSC predicted monthly A_p envelope.

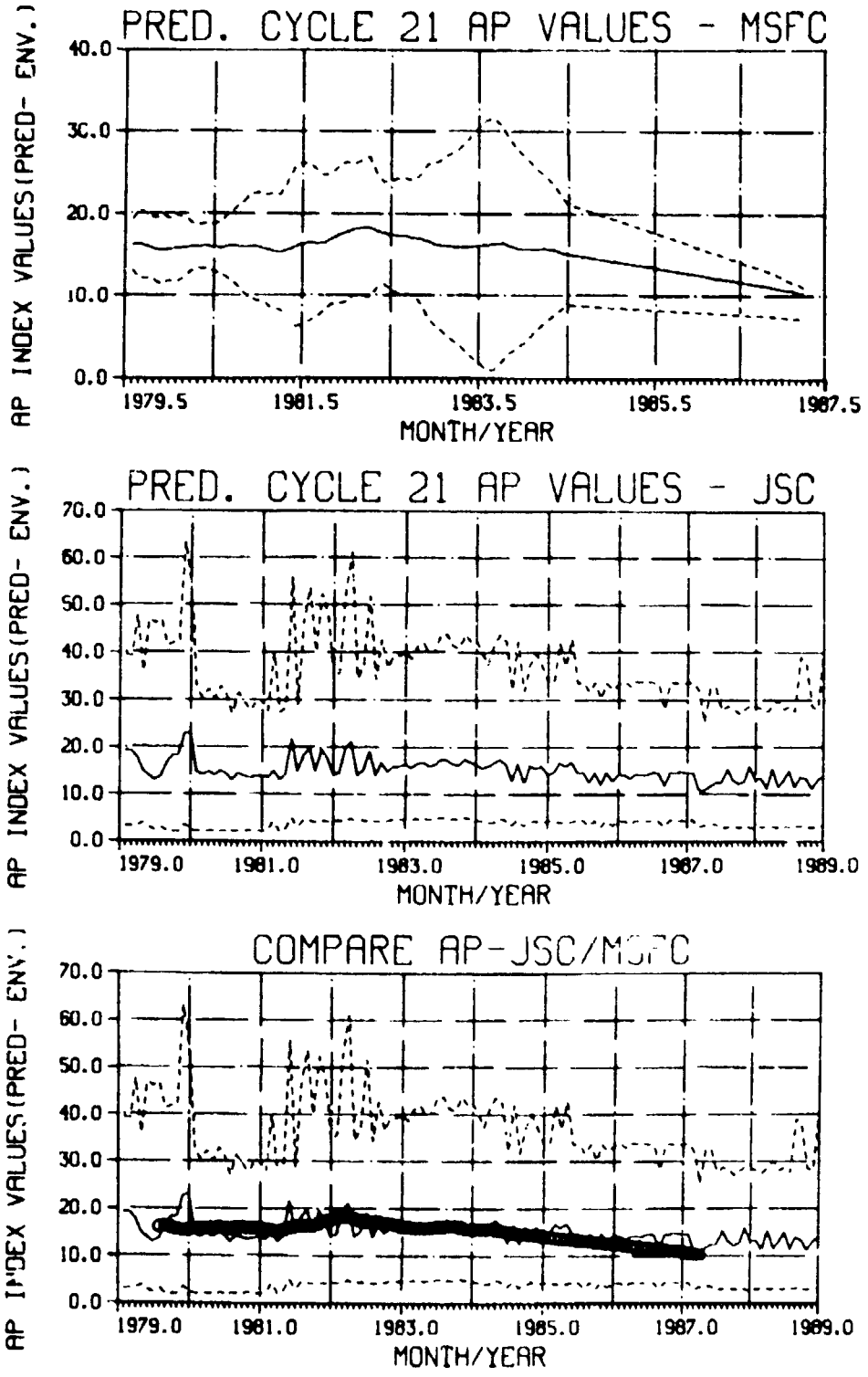

Figure 30.- Summary plots of the MSFC and JSC A_p envelopes.

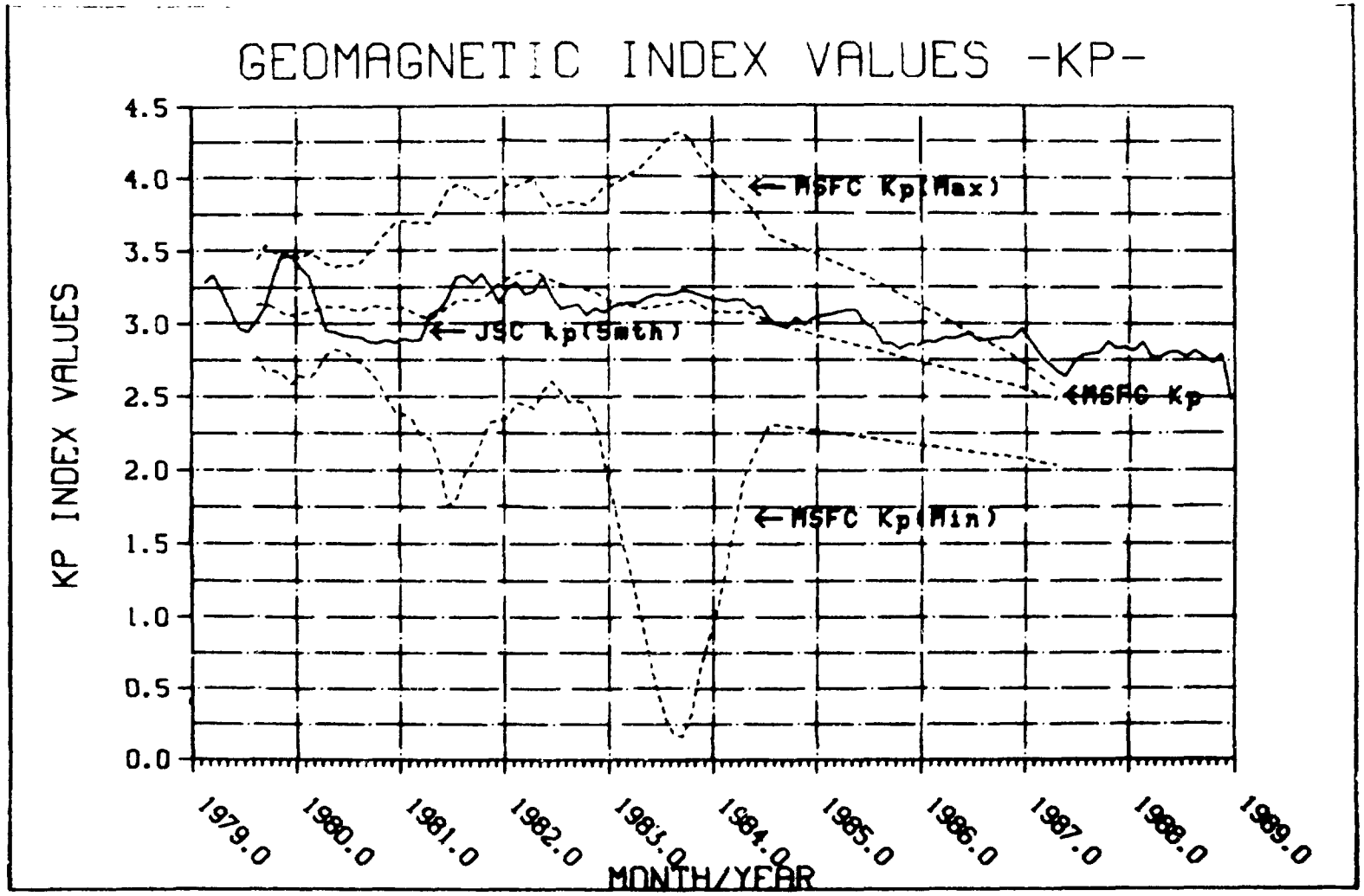

Figure 31.- Predicted MSFC 5-month K_p envelope and JSC 5-month K_p average values (1979-1989).

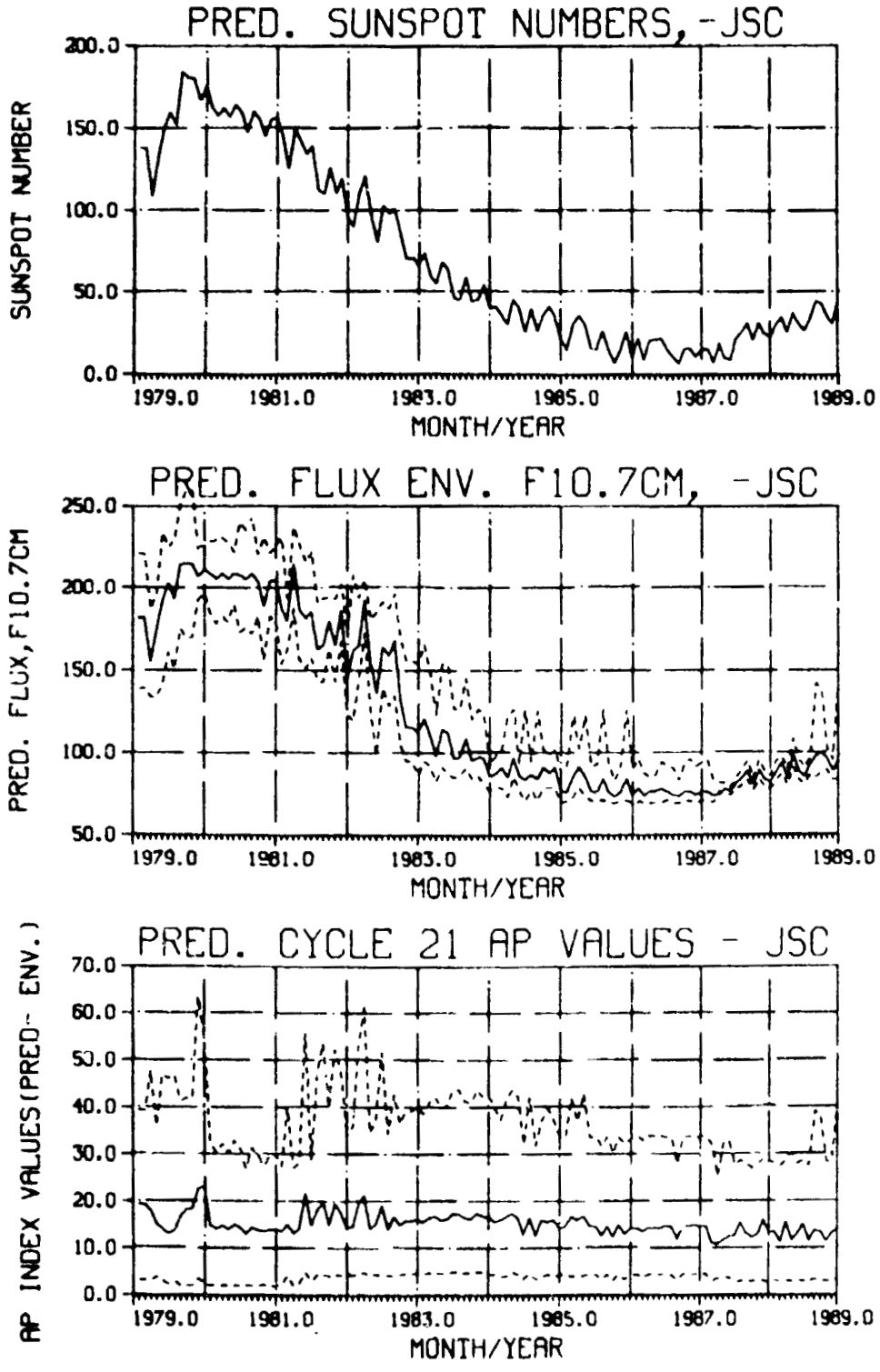

Figure 32.- Summary plots of predicted sunspot numbers, predicted solar flux (F10.7 cm), and predicted A_p values (1979-1989).

U S GOVERNMENT PRINTING OFFICE 1980-671 099/2240